



**WEAR ANALYSIS OF CU-AL COATING ON  
TI-6AL-4V UNDER FRETTING**

THESIS

Karl N. Murray, Ensign, USN  
AFIT/GAE/ENY/06-J12

**DEPARTMENT OF THE AIR FORCE  
AIR UNIVERSITY**

**AIR FORCE INSTITUTE OF TECHNOLOGY**

**Wright-Patterson Air Force Base, Ohio**

APPROVED FOR PUBLIC RELEASE; DISTRIBUTION UNLIMITED

The views expressed in this thesis are those of the author and do not reflect the official policy or position of the United States Air Force, Department of Defense, or the United States Government.

AFIT/GAE/ENY/06-J12

WEAR ANALYSIS OF CU-AL COATING ON TI-6AL-4V UNDER FRETTING

THESIS

Presented to the Faculty

Department of Aeronautic and Astronautics

Graduate School of Engineering and Management

Air Force Institute of Technology

Air University

Air Education and Training Command

In Partial Fulfillment of the Requirements for the  
Degree of Master of Science in Aeronautical Engineering

Karl N. Murray, BS

Ensign, USN

June 2006

APPROVED FOR PUBLIC RELEASE; DISTRIBUTION UNLIMITED.

AFIT/GAE/ENY/06-J12

WEAR ANALYSIS OF CU-AL COATING ON TI-6AL-4V UNDER FRETTING

Karl N. Murray, BS  
Ensign, USN

Approved:



5/25/06

---

Dr. Shankar Mall (Chairman)

---

date



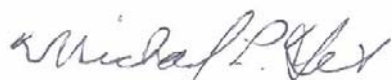
5/25/06

---

Dr. Vinod K. Jain (Member)

---

date



5/31/06

---

Dr. Michael L. Heil (Member)

---

date

### **Acknowledgments**

I would like to thank Dr. Shankar Mall for his help in guiding me and providing suggestions throughout the entire process; Dr. Mall was also a great teacher of structures. Dr. Hyukjae Lee's help was also very beneficial; his experience in performing fretting tests was crucial in helping me to set up and carry out my experimental testing. Dr. Russell Magaziner's assistance in setting up my testing was also very valuable. I would also like to thank Mr. Barry Page for teaching me to use the laboratory equipment and fixing the various things I broke during the learning process.

Karl N. Murray

## **Table of Contents**

	Page
Acknowledgments.....	iv
Table of Contents.....	v
List of Figures.....	vii
List of Tables .....	viii
Nomenclature.....	ix
Abstract.....	xi
I. Introduction .....	1
1.1 Coating Method:.....	1
1.2 Explanation of Wear Categories:.....	2
1.3 Experimental Setup: .....	3
II. Background Information .....	4
2.1 Fretting Test Setup: .....	4
2.1.1 Explanation of Different Fretting Regimes:.....	5
2.2 Summaries of Previous Works: .....	5
2.2.1 Ren, Mall, Sanders, and Sharma [17]: .....	5
2.2.2 Ren, Mall, Sanders, and Sharma [16]: .....	6
2.2.3 Jin, Mall, Sanders, and Sharma [11]: .....	6
2.2.4 Jin, Mall, Sanders, and Sharma [10]: .....	7
2.2.5 Lee, Mall, Sanders, and Sharma [12]:.....	7
2.3 Current Study: .....	8
2.3.1 Peak Pressure Matching:.....	9
2.3.2 Relative Displacement Calculations: .....	10
III. Experiments .....	13
3.1 Specimen Data:.....	13
3.2 Experimental Setup: .....	13
3.2.1 Setups from Previous Studies: .....	13

	Page
3.2.1.1 Lee [12]:.....	14
3.2.1.2 Magaziner [14]:.....	14
3.2.2 Setup for Current Study: .....	14
3.3 Experimental Procedure: .....	16
3.3.1 Fretting Tests:.....	16
3.3.2 CoF Measurements:.....	17
3.3.3 Wear Volume Measurements: .....	18
IV. Results and Discussion .....	29
4.1 Fretting Loops: .....	29
4.1.1 Fretting Regime:.....	30
4.2 Wear Analysis: .....	31
4.2.1 Accumulated Relative Displacement Method:.....	31
4.2.2 Accumulated Dissipated Energy Method: .....	32
4.2.2.1 Normalized Wear Depth: .....	34
4.2.2.2 Tangential Force: .....	35
V. Conclusions.....	49
5.1 Summary of Problem:.....	49
5.2 Summary of Results: .....	49
5.3 Knowledge Gained from Study: .....	50
VI. Future Work .....	52
6.1 Tests with Longer Extensometer Gauge Length: .....	52
6.2 Data Points Recorded per Cycle:.....	53
6.3 SEM Analysis: .....	53
Appendices.....	55
Bibliography .....	60
Vita.....	62

## List of Figures

Figure	Page
Figure 2.1 Contact Zones .....	11
Figure 2.2 Extensometer Setup .....	12
Figure 3.1 Specimen Dimensions .....	20
Figure 3.2 Test Setup with Lubricating System .....	21
Figure 3.3 Fretting Machine Setup .....	22
Figure 3.4 Extensometer Setup .....	23
Figure 3.5 Typical Fretting Scar (Test 5) .....	24
Figure 3.6 Profilemeter Measurement of Surface (Test 1) .....	25
Figure 3.7 Profilemeter Measurement of Surface (Test 7) .....	25
Figure 3.8 Three-Dimensional Surface Profile (Test 1) .....	26
Figure 3.9 Three-Dimensional Surface Profile (Test 7) .....	27
Figure 4.1 Typical Fretting Loops of Partial Slip (Test 1) .....	38
Figure 4.2 Typical Fretting Loops of Gross Slip (Test 4) .....	39
Figure 4.3 Typical Fretting Loops of Mixed-Mode (Test 5) .....	40
Figure 4.4 Fretting Loops at the 15,000 <sup>th</sup> Cycle for Each Test (No Fatigue) .....	41
Figure 4.5 Fretting Loops at the 15,000 <sup>th</sup> Cycle for Each Test (Fatigue) .....	42
Figure 4.6 Accumulated Relative Displacement Range vs. Wear Volume .....	43
Figure 4.7 Accumulated Dissipated Energy vs. Wear Volume .....	44
Figure 4.8 Close-in View of Accumulated Energy for Current Study .....	45
Figure 4.9 Normalized Wear Depth vs. Accumulated Dissipated Energy .....	46
Figure 4.10 Tangential Force vs. Number of Cycles .....	47

## **List of Tables**

Table	Page
Table 3.1 Program of Experimental Tests .....	28
Table 4.1 Data Summary for Current Study .....	48
Table 4.2 Data Summary for Lee Study [12].....	48

## Nomenclature

2a	contact width
A	specimen cross sectional area
CoF	coefficient of friction
F	fatigue load
E	modulus of elasticity
N	number of cycles
P	normal load
$p_o$	peak contact pressure
$p(x)$	normal pressure distribution
k	relative radius of curvature
$l_{AB}$	distance between the center of the contact region and the upper arm of the extensometer
$l_{DC}$	distance of the extensometer from the specimen surface
Q	tangential, frictional force
R	pad radius
x	distance along the specimen surface from the center of contact
$\alpha$	constant that is related to the compliance of the fretting fixture
$\delta$	relative displacement between specimen and pad at the center of contact
$\delta_{AB}$	vertical displacement between the center of contact and the upper extensometer arm
$\delta_{EXT}$	displacement measured by the extensometer
$\delta_{DC}$	displacement due to the compliance of the fretting fixture

v

Poisson's ratio

x

## Abstract

The effects of changes in the coefficient of friction (CoF) between the contacting surfaces on the fretting wear characteristics of Cu-Al coating on Ti-6Al-4V were investigated. This Cu-Al coating is part of a system that is applied to titanium turbine blades to reduce fretting at the interface. In the application, there is a solid lubricant that is added on top of the coating as an assembly aid and to help reduce the friction while the lubricant remains within the contact. Previous studies have researched the characteristics of the coating without the additional lubricant. In this study, liquid motor oil was applied to the contact region to simulate real-world conditions with a lower CoF. To characterize the wear, several methods were used, the most useful being the accumulated dissipated energy method. The accumulated relative displacement method did not take into account the differences between the tangential forces for tests conducted at different CoF values, whereas the dissipated energy method did. The wear characteristics of tests conducted in the current study were similar to those of a previous study, conducted at a higher CoF, when analyzed with the dissipated energy method, but this was most likely due to the ambiguity of the calculated wear volumes.

# WEAR ANALYSIS OF CU-AL COATING ON TI-6AL-4V UNDER FRETTING

## I. Introduction

Fretting is a major problem for the aircraft of our nation's military. Fretting arises when two materials are in contact under pressure and small-scale relative motion occurs between them. The damage from fretting can be caused either by fatigue of one or both of the contacting materials or from wear, in which enough of the contacting material is worn away such that the object no longer fits into its specific configuration and no longer functions properly. The gas turbine engines installed on airplanes have a major source of fretting, specifically, in the dovetail joint at the disk-blade attachment in the engine. Because it has a high strength-to-weight ratio and strong temperature performance, a titanium alloy, Ti-6Al-4V, is commonly used in many aerospace components, including the dovetail joints of a gas turbine engine. Though strong, Ti-6Al-4V is susceptible to fretting fatigue and wear, and limiting the damage of the titanium and failure of the dovetail joints is very important. Decreasing the damage from fretting in the dovetail joints will help to decrease the maintenance work required on the gas turbine engines and increase the lifespan of our nation's military aircraft.

### 1.1 Coating Method:

The ultimate goal of the global fretting research that has been previously undertaken and is currently being conducted is to eliminate and or decrease the damage from fretting fatigue. Several methods have been researched in attempts to decrease fretting damage such as shot peening the titanium before it is subjected to fretting [21]. Application of a solid coating is another method. The specific goal of the research in this

study was to analyze the fretting wear of a metallic coating, Cu-Al, that had been applied to a titanium substrate. Application of a metallic coating to one or both of the surfaces that are undergoing relative motion can help to prevent fretting fatigue and wear. If the metallic coating is soft (has a low yield stress), movement between the two surfaces may be taken up in the coating. The coating must be able to withstand very severe fatigue and wear and must adhere strongly to the substrate [19]. Cu-Al coating is one type of soft metallic coating that has been demonstrated to potentially decrease fretting damage. Care must be taken when applying the coating to the substrate; cracks or flaws in the coating can act as stress raisers, and a fatigue crack initiated in the coating will usually propagate into the underlying substrate material [19].

### 1.2 Explanation of Wear Categories:

Wear is defined as the removal of a small amount of material from solid surfaces as a result of mechanical action [15]. There are two main types of wear: adhesive wear and abrasive wear [15, 19]. Adhesive wear occurs when two smooth bodies slide over each other and fragments are pulled off one surface and adhere to the other. Adhesive wear is the most common type of wear but is also the least preventable. When any two surfaces are brought in contact and are then separated, either in the tangential or normal direction, there is a tendency, from attractive forces, for material to be pulled from one surface to another.

Abrasive wear occurs when a surface slides on a softer surface and creates a series of grooves in it that generate a relatively large amount of debris. If the hard surface can be made very smooth, with a coating or lubrication, it is possible to eliminate

abrasive wear. High microhardness of the coating is required to resist the abrasion-wear mechanisms—if relative displacement between two materials (one hard and one soft) takes place, it is possible for abrasive wear to occur and for the harder surface to completely wear away the softer surface [1]. In the case of this study, the harder Ti-6Al-4V fretting pads can completely wear away the softer Cu-Al coating.

### 1.3 Experimental Setup:

The real-world conditions that take place in a turbine engine are very complex. The purpose of the experimental setup in this study was to simulate those conditions with some simplifications to analyze the wear of a coating that can be utilized to prevent fretting damage of the dovetail joints in a turbine engine. A test rig created in the Air Force Institute of Technology materials laboratory was used to simulate the same conditions using a servo-hydraulic test machine, specially designed fretting pads, and a fretting fixture. In actual turbine engines, there is a solid lubricant that is added on top of the coating to reduce the friction. In the current study, this was simulated by conducting the tests under lubricated conditions with the application of motor oil to the contact area. Though the setup introduces many simplifications, it is the hope that a better understanding of the fretting wear of the Cu-Al coating under lubricated conditions will be gained that can be applied to the real world.

## II. Background Information

The environment inside a gas turbine engine is very complex, and simulating the conditions in which the turbine blades operate is very difficult. Some simplifications must be made to model these turbine blades so that analysis of possible failure mechanisms may be investigated. The size, shape, and material characteristics of the turbine blades are not only a structural matter, but also an aerodynamic matter, and their design is a very complicated and iterative process.

The use of a coating system for the blades is one possible solution to improve the life endurance of the blades. A series of studies have been undertaken to research different coating systems in a simplified laboratory setting to determine the effect of the coating systems on fretting wear and fatigue [10, 11, 12, 16, 17]. From previous research [17], it has been found that a soft coating is better for preventing fatigue damage because the softer coating acts as a solid lubricant, which can subsequently reduce friction and hinder cracking from fretting fatigue. A hard coating, on the other hand, is better for preventing damage from fretting wear.

### 2.1 Fretting Test Setup:

For the purposes of this study, cylindrical fretting pads were used, which results in a Hertzian pressure distribution on the specimen—when pressure is exerted on the specimen from the pad, the materials compress and flatten together in a plane [19]. The length of the specimen that is actually touching the cylindrical pad is known as the

contact width,  $2a$ . Fretting occurs when the specimen is stretched and a tangential force,  $2Q$ , is applied from the cylindrical pads to the specimen.

### 2.1.1 Explanation of Different Fretting Regimes:

Within the contact area for most fretting experiments, there are typically three different regions. The center area, the stick zone, is where the pad and specimen stick together. On both sides of the stick zone are regions, the slip zones, where the pad and specimen slip relative to each other. Outside of the slip zones, the pad and specimen are no longer in contact. These three zones can be seen in Figure 2.1.

In this study, two principal fretting regimens were studied: partial and gross slip. For the partial slip regimen, the pad and specimen initially stick together with slip regions. For the gross slip regimen, there is no longer any stick zone—the pad and specimen are constantly sliding against each other; the only contact region that is present is the slip zone.

### 2.2 Summaries of Previous Works:

This study is a continuation of the following studies that have been performed at the Air Force Institute of Technology over the last several years, so they will be discussed briefly to provide the background of the present study.

#### 2.2.1 Ren, Mall, Sanders, and Sharma [17]:

In the first of the series of previous studies, four different coating systems,  $TiCn$ ,  $CrN+MoS_2$ ,  $Cu-Al$ , and  $Ag^+$ , were analyzed for their potential to improve fatigue

behavior of Ti-6Al-4V. In this study, there appeared to be no improvement in fretting fatigue life from any of the coating systems, as compared with the uncoated specimen tested; this was due to preexisting flaws introduced during the coating process. The Cu-Al coating served as a lubricating agent; with an increase in the fretting fatigue cycles, the rough surface of the specimen became smoother because more debris were generated from the fretting motion. Thus, based on this study, Cu-Al coating showed the most promise for decreasing fretting fatigue.

#### 2.2.2 Ren, Mall, Sanders, and Sharma [16]:

In this study, the wear and the CoF of the Cu-Al coating on Ti-6Al-4V substrate were analyzed. The results showed that, as the fretting cycles increased, the CoF decreased to a certain value until the Cu-Al coating was worn out—at which point the CoF was the same as that for the bare substrate. The decrease in the CoF was due to the self-lubrication of the debris generated during fretting. From this study, it was determined that an improvement in fretting fatigue life was linked with a degradation of the coating, providing evidence that a slower degradation would be more beneficial for improving fretting fatigue life.

#### 2.2.3 Jin, Mall, Sanders, and Sharma [11]:

In still another study, Cu-Al coating was analyzed at different bulk-stress amplitudes under a constant contact load and at different contact loads under a constant bulk-stress amplitude; the results were compared against bare Ti-6Al-4V substrate specimens. For lower contact loads, gross slip was the predominant fretting regimen, and

the coating life suffered the most as a result of the high fretting wear related to this regimen. Building upon previous studies that had found that an increase in coating life improves fretting fatigue life, the results of this study determined that coating life increased with increasing contact load. Wear damages the coating that provides protection to the titanium substrate from fretting fatigue. Fretting wear must be further studied to determine factors that can reduce the wear and increase the lifecycle of the titanium substrate.

#### 2.2.4 Jin, Mall, Sanders, and Sharma [10]:

This was a continuation of a previous study [11] to determine the durability and causes of degradation of the Cu-Al coating on the Ti-6A-4V substrate. In the previous study, it was established that an increase in contact load decreased the wear of the coating; in this study, the contact load was kept constant, and different stress amplitudes were applied. In both this and the previous study, the CoFs of the coated and uncoated substrate were compared both before and after fretting—before fretting, the coated substrate showed a lower CoF, whereas after exposure to fretting, both the coated and uncoated specimens had approximately the same CoF. As the applied stress amplitudes were increased, the coating eventually separated from the substrate as the result of insufficient interfacial strength.

#### 2.2.5 Lee, Mall, Sanders, and Sharma [12]:

This study was a continuation of the Jin study [10] and specifically studied the wear of the Cu-Al coating on the Ti-6Al-4V substrate. This study attempted to characterize the wear by measuring dissipated energy in different fretting regimens, including both the partial slip and gross slip conditions. In this study, wear damage was

characterized using two different methods: comparing the wear volume against both the total dissipated energy and accumulated relative displacement range. It was found that there was a linear relationship between both the wear volume and accumulated dissipated energy and between the wear volume and accumulated relative displacement. Tests were run with varying applied displacements both with and without an applied fatigue load. Only when a large value of displacement was applied did the wear in the substrate material occur beyond the thickness of the Cu-Al coating.

Under this study's fretting conditions, the Cu-Al coating debris remained at the contact surface throughout testing and characterized abrasive wear—the generation of wear debris was greater than the removal of debris from the contact surface that caused an increase in tangential force (until an equilibrium was reached) as the test cycles progressed. This study concluded that an accumulated relative displacement range method is a feasible alternative method for wear analysis of soft materials. In broader terms, this study also showed the possibility that a softer coating, such as Cu-Al, could do more damage to a harder substrate, such as Ti-6Al-4V, under certain fretting conditions, such as that of this study.

### 2.3 Current Study:

If relative movement between two surfaces must occur, one possible method of preventing fretting damage is to create conditions so that there is as low a CoF as possible. In this study, the effect of decreasing the CoF on fretting wear of the Ti-6Al-4V substrate with Cu-Al coating was analyzed. In modern gas turbine engines, lubricant is applied to the moving part to decrease the CoF. The same test conditions used in Lee

[12] were replicated in this study, with oil being applied throughout the test cycles to lower the CoF.

### 2.3.1 Peak Pressure Matching:

For the current study, it was important to match the parameters used in Lee's study [12] so that the effect of changing the CoF could be independently studied. One parameter that had to be matched was the Hertzian peak pressure [13].

The normal pressure distribution is given as:

$$p(x) = p_o \left( 1 - \left( \frac{x}{a} \right)^2 \right)^{\frac{1}{2}} \quad (1)$$

The peak pressure is given as:

$$p_o \frac{2P}{\pi * a} \quad (2)$$

where

$$P = \frac{\pi * k * a^2}{2A^*} \quad (3)$$

and

$$k = \frac{1}{R} \quad (4)$$

$$A^* = 4 \left( \frac{1 - \nu^2}{E} \right) \quad (5)$$

### 2.3.2 Relative Displacement Calculations:

The Wittkowsky study [19] developed a successful procedure to measure the relative displacement at the center of contact between the specimen and fretting pads—it was this procedure that Lee and colleagues used [12] and that is being employed in the current study. Before the Wittkowsky study, a variety of procedures had been used to measure displacement between the contact surfaces, but the procedure developed by Wittkowsky ultimately became the standard for fretting-fatigue research. The equations developed to measure the relative displacement are given as follows:

$$\delta = \delta_{AB} - (\delta_{EXT} + \delta_{DC}) \quad (6)$$

$$\delta_{AB} = \left( \frac{F - 2Q}{AE} \right) l_{AB} \quad (7)$$

$$\delta_{DC} = -\alpha * Q * l_{DC} \quad (8)$$

$l_{AB}$  is the measured distance between points A and B, and  $l_{DC}$  is the distance between points D and C on Figure 2.2.

The constant  $\alpha$  is directly related to the compliance of the fretting fixture, and the value used in both this experiment and in Lee's work [12] was determined from previous experiments using the same test rig and fretting fixture; two quasi-static tests were conducted in which the value of  $l_{DC}$  was changed but the value of Q in both tests was kept constant [8]. The equation to calculate  $\alpha$  is given below:

$$\delta_{EXT1} - \alpha * l_{DC1} * Q = \delta_{EXT2} - \alpha * l_{DC2} * Q \quad (9)$$

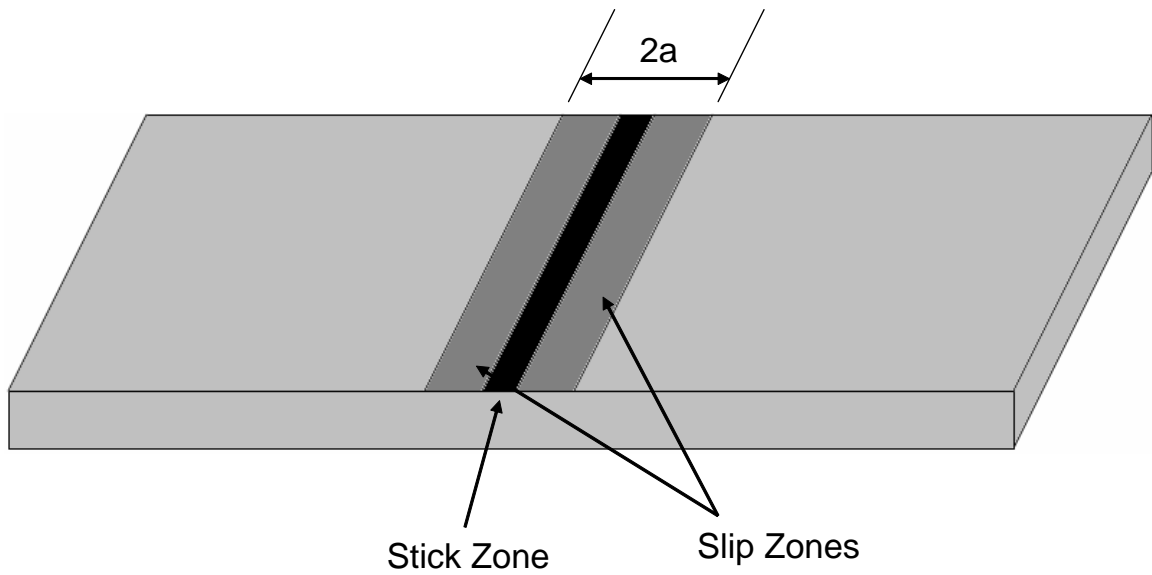


**Figure 2.1 Contact Zones**

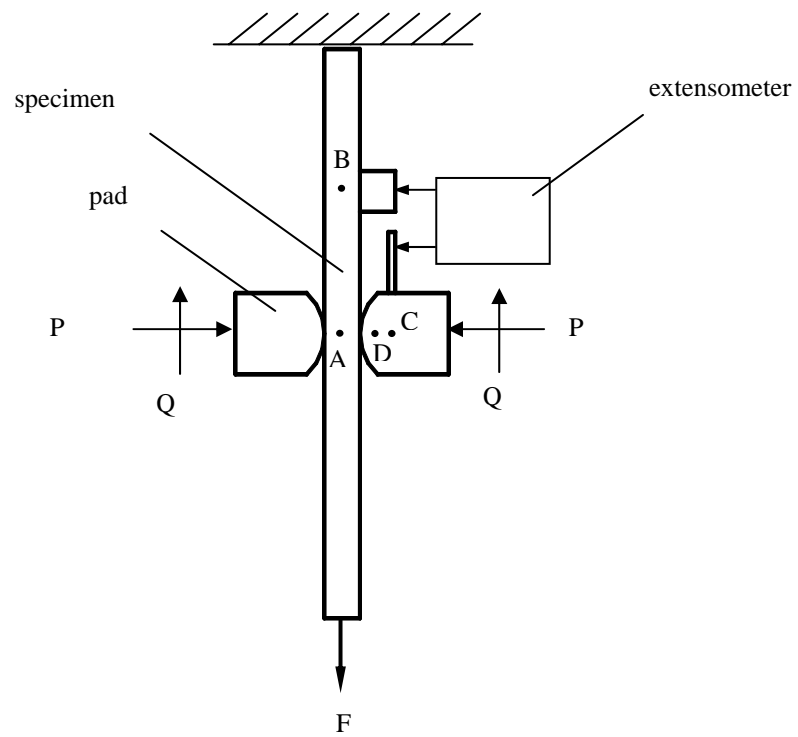


**Figure 2.2 Extensometer Setup**

### **III. Experiments**

#### 3.1 Specimen Data:

The specimen substrate was a titanium alloy, Ti-6Al-4V. Before the material was machined, it was preheated and solution treated at 935°C for 105 minutes, cooled in air, vacuum annealed at 705°C for 2 hours, and then cooled in argon. The microstructure of the material was comprised of two phases: 60% volume of  $\alpha$  (HCP) and 40% of  $\beta$  (BCC), with the nucleation of the  $\alpha$  plates in the  $\beta$  matrix. The grain size was approximately  $10 \mu\text{m} \pm 2 \mu\text{m}$ . The material has an elastic modulus of 126 GPa, yield strength of 930 MPa, and ultimate tensile strength of 978 MPa. The final dimensions of the specimen (see Figure 3.1) after cutting with the wire electrical discharge method and low stress grinding (to reduce residual machining stress) were a length of 17.78 cm, width of 0.64 cm, and thickness of 0.38 cm, which gave a cross-sectional area of  $0.24 \text{ cm}^2$ . The cylindrical fretting pads were machined from the same Ti-6Al-4V material and had a radius of 0.3 cm. The Cu-Al coating was applied to the specimen by plasma spray method. The composition of the coating was 87 ~ 90 wt% of Cu, 9 ~ 11 wt% of Al, and 0.7 ~ 1.5 wt% of Fe. The average thickness of the Cu-Al coating was measured by profilemeter and was determined to be 40  $\mu\text{m}$ . The root mean square (RMS) surface roughness of both the specimen substrate and the pad was 0.2  $\mu\text{m}$ .

#### 3.2 Experimental Setup:

##### 3.2.1 Setups from Previous Studies:

The setup used for experimental testing in this study was created based on past studies that researched fretting performed at the Air Force Institute of Technology. The profilemeter used to make surface measurements was a new piece of equipment that had not been used in previous studies.

#### 3.2.1.1 Lee [12]:

Fretting tests in this study were performed using the servo-hydraulic uniaxial test frame with an additional servo-hydraulic actuator at the Air Force Institute of Technology. Fretting tests were performed with either no fatigue load or at the maximum fatigue stress of 300 MPa, with a stress ratio of 0.1. The applied pad displacement was varied for each test. All tests were run up to 15,000 cycles at a frequency of 2 Hz. The applied contact load was 320 N, which resulted in a Hertzian peak pressure of 615 MPa.

#### 3.2.1.2 Magaziner [14]:

In this study, the same dual-actuator fretting machine used in the current study had been used. In this study, the effects of the variation in CoF on the critical contact width were analyzed. A series of tests were performed in which oil was dropped in a controlled manner, at a flow rate of 5.5 E-3 ml/s, into the contact area. See Figure 3.2 for a diagram of the test rig used to lubricate the specimen.

#### 3.2.2 Setup for Current Study:

The focus of this study was to determine the effect that the CoF of the coating had on the change in fretting wear of the Ti-Al-4V substrate. To do this, tests similar to those run in Lee [12] were replicated, with the only difference being the change in the CoF of

the coating. The static CoF of the specimen for both the dry and lubricated states was also determined using the same dual-actuator machine used to run the fretting tests.

Fretting tests were performed on a dual-actuator fretting machine located in the Air Force Institute of Technology Materials Laboratory. The machine was controlled using *MTS TestStar II* computer software on a basic desktop computer. All the tests were performed under room temperature and normal pressure conditions. For a portion of the tests, the specimen was put under a varying fatigue load, whereas, for some tests, the specimen was simply held in a fixed position. The testing apparatus allowed the specimen to be held in place by an upper grip while the lower grip could be moved to induce various fatigue loads on the specimen. At the same time that the lower grip actuator was moving, an upper actuator was used to move a fretting fixture placed about the specimen.

Factors that were the same as those used by Lee [12] were the applied contact load of 320 N, the fatigue stress of 300 MPa with a stress ratio of 0.1, and the same overall testing method—which included the technique of measuring the relative displacement using the same extensometer setup. The force applied by the lower actuator to achieve the desired fatigue load was calculated by multiplying the specimen's cross-sectional area by the desired pressure.

To change the CoF, oil was applied to the specimen throughout the test cycles using a setup very similar to that used by Magaziner [14], as depicted in Figure 3.2. In actual turbine engines, a lubricating system is used to apply oil to the blades, which then reaches the dovetail joints; therefore, it was assumed that this would be a fairly accurate method to use to replicate real-life conditions. SAE 15W-40 Heavy Duty Motor Oil was

used in this experiment. Though it is not exactly the same oil as is used in the aerospace industry and gas turbine engines, its lubricating properties are similar and suffice for the simplification of this laboratory testing.

### 3.3 Experimental Procedure:

#### 3.3.1 Fretting Tests:

The specimen was placed vertically in the upper and lower grips of the servo-hydraulic test frame and gripped on the top and bottom with a grip pressure of 2,000 psi. Fretting pads were then placed in slots on the upper fretting frame and set in place (see Figure 3.3)—new fretting pads were used for each experimental test. The fretting pads were forced against the specimen with the desired contact load, which could be measured by a load cell. Before each test was run, the alignment of the fretting pads against the specimen was verified by placing pressure-sensitive tape on the specimen and pressing the fretting pads against the specimen with the desired contact load.

Once the specimen was in place with the fretting pads forced against it with the desired contact load, the extensometer had to be set up to measure the relative displacement, as discussed in section 2.5. In the Lee study [12], an extensometer with a gauge length of 0.5 in. was used; unfortunately, this extensometer was not available for use in the current study. For the current study, an extensometer with a gauge length of 0.3 in. was used. A piece of metal was glued onto the top of the fretting frame with a slot for the bottom knife edge of the extensometer to fit into. Another piece of metal was clamped onto the titanium specimen for the top knife edge of the extensometer to fit into (see Figure 3.4). The extensometer was fitted into the designated slots and then held in

place with rubber bands—rubber bands were used so that if the extensometer was stretched to its limit, the bands would break without damaging the extensometer.

With the extensometer attached and the specimen gripped, the lubricating system was set up to get oil onto the specimen and pads to lower the CoF. Oil was brought from an upper reservoir, which had been placed above the testing frame. Small capillary tubes were used so that oil could be dripped above where the pads contacted the specimen to ensure that oil entered into the contact area and that both the pads and specimen were lubricated (see Figure 3.2).

Once the specimen was aligned properly, the extensometer was attached, and the lubricating system was running, the next step was to actually run the experiments; the program of experimental tests can be seen in Table 3.1. The testing procedures were run using *MTS TestStar II* computer software. For each test, a displacement was applied with the upper actuator moving the fixture with the pads to induce fretting on the specimen. Two types of tests were run—tests with a fatigue load, and tests without a fatigue load. For tests that did not have a fatigue load, the lower grip was held in place; for tests that did have a fatigue load, the lower actuator (labeled Actuator 1 in Figure 3.3) was used to move the lower grip, inducing a fatigue load ( $F$ ) in the specimen. Each test was run to 15,000 cycles at a frequency of 2 Hz.

### 3.3.2 CoF Measurements:

The static CoFs for the specimen in the dry and lubricated conditions were measured using the dual servo-hydraulic test frame. The specimen was gripped on the top and bottom to ensure it was aligned vertically. A contact force was then applied with

the fretting pads—in this case, a contact force of 320 N was used. The extensometer was setup and attached in the same method as was used for the fretting tests. The upper grip was than released and a force was applied to the lower actuator until the specimen started to slip. The extensometer readings were used to determine exactly when slip started to occur. The force from the lower actuator used to induce slip was recorded. Several tests were conducted in each condition, and the CoF was determined from an average of these tests—the CoF was determined by dividing the average value of the tangential force during slip by the applied normal load to the fretting pad. The static CoF for the dry condition was determined to be  $\sim 0.24$ , and the static CoF for the lubricated condition was  $\sim 0.13$ .

### 3.3.3 Wear Volume Measurements:

After testing, the titanium specimen was cleaned. The specimen was put into a sonication cleaning machine filled with ethanol alcohol, and the sonication process was allowed to run for one hour. Two-dimensional surface profiles were created for each fretting scar using a profilemeter. The scar was scanned from one side to other in the x-direction, at seven different locations spaced 1 mm apart in the y-direction (see Figure 3.5). Unfortunately, the profilemeter used in the current study was not the same as that used in the Lee study [12], which could result in differences between how accurate the wear area measurements in this study are, as compared with Lee's measurements.

The wear area was calculated for each two-dimensional surface profile using *Taylor Hobson* computing software, knowing the wear length and depth (see Figure 3.6 and Figure 3.7). It was possible to numerically integrate the wear-area data for the seven

different locations spaced evenly along the width of the scar to determine the total wear volume of the scar. From the two-dimensional data collected for each fretting scar, three-dimensional surface profiles were created that were a numerical approximation of the actual fretting scars (see Figure 3.8 and Figure 3.9). The wear volume was calculated using Simpson's Rule:

$$Volume = \int_a^b f(x)dx = \frac{h}{3} [f(x_0) + 4f(x_1) + 2f(x_2) + 4f(x_3) + 2f(x_4) + 4f(x_5) + f(x_6)] \quad (10)$$

Where  $h$  = the distance between each measurement (in this case, 1 mm), and  $f(x_i)$  = area for the  $i^{\text{th}}$  surface profile.

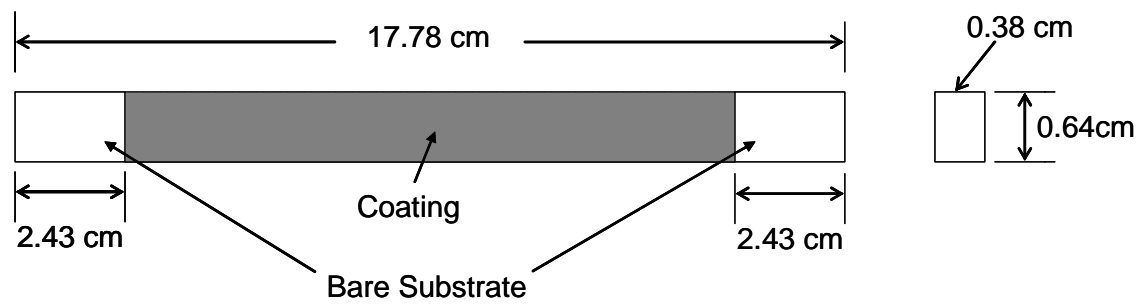


**Figure 3.1 Specimen Dimensions**

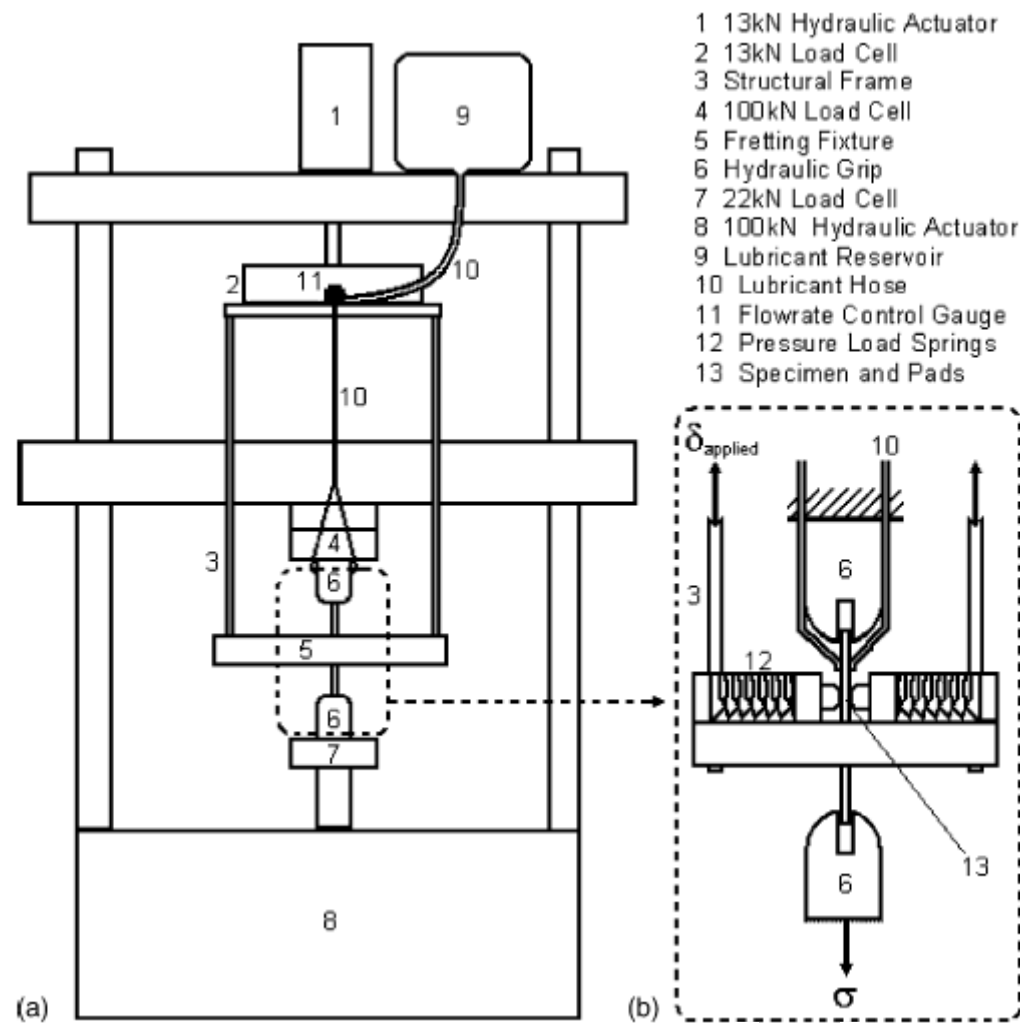
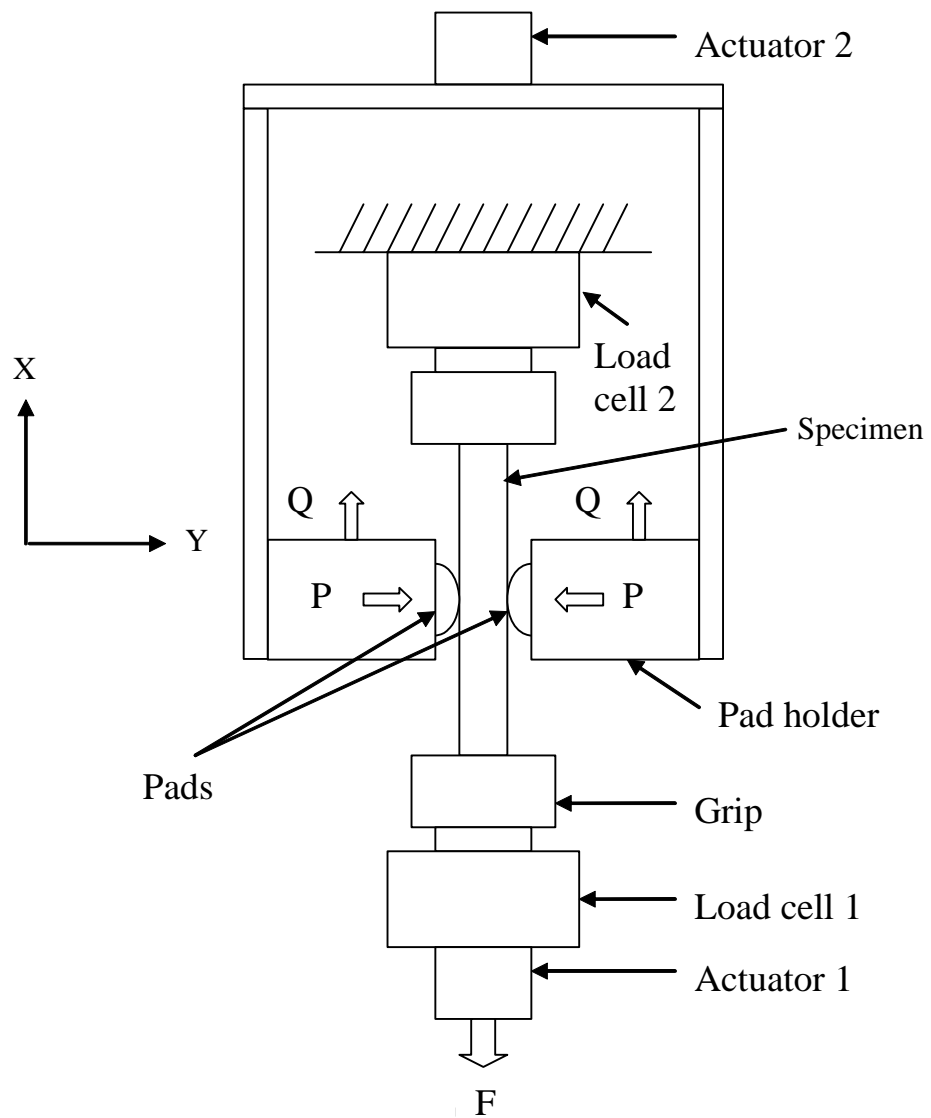
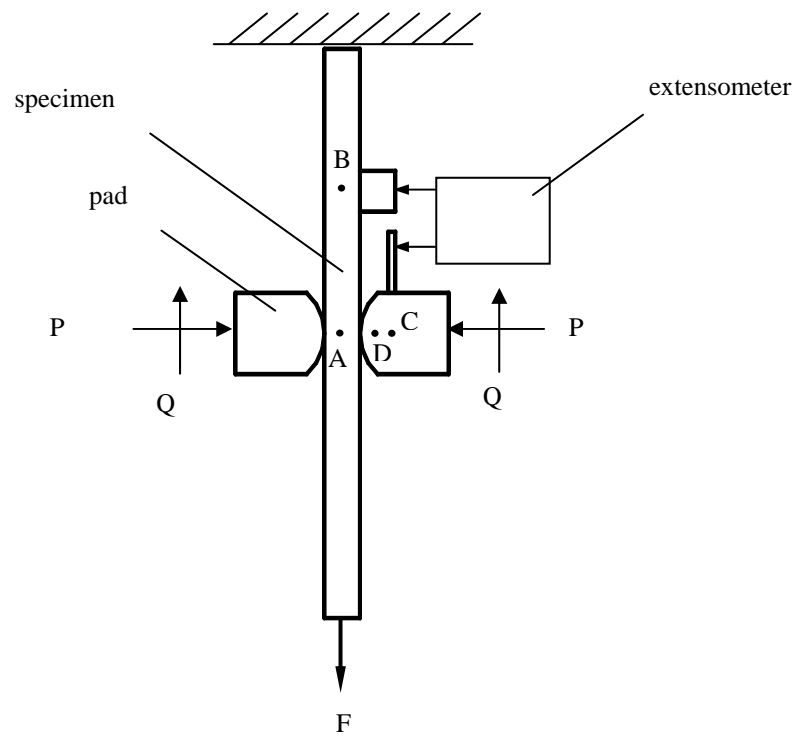


Figure 3.2 Test Setup with Lubricating System



**Figure 3.3 Fretting Machine Setup**



**Figure 3.4 Extensometer Setup**

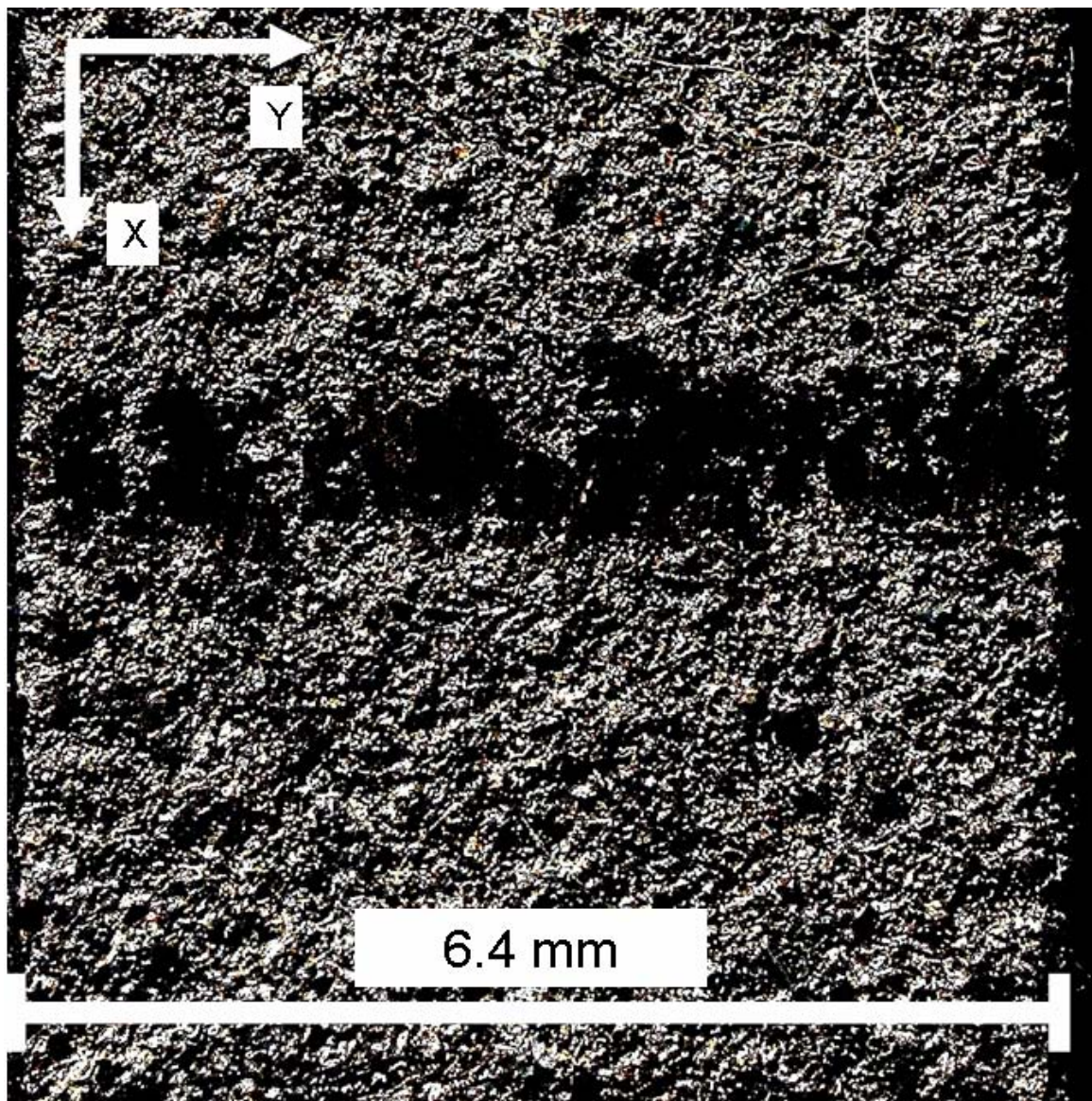
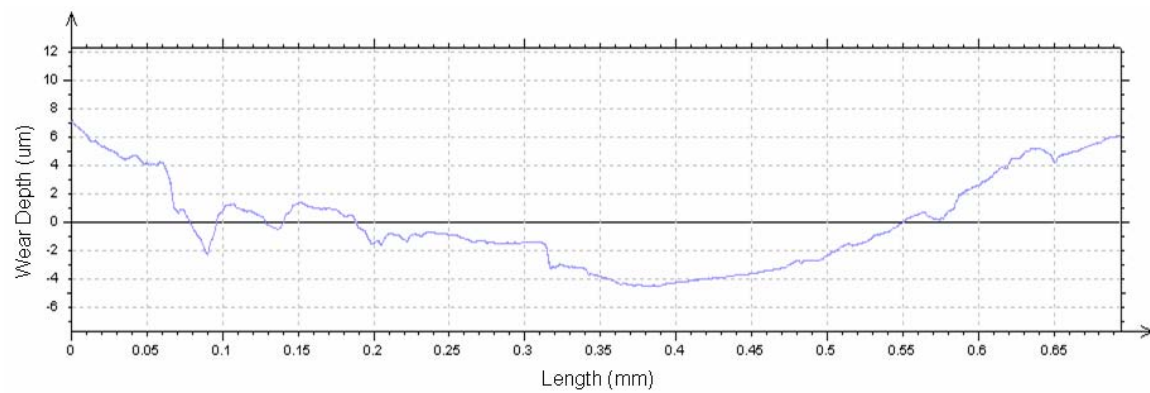
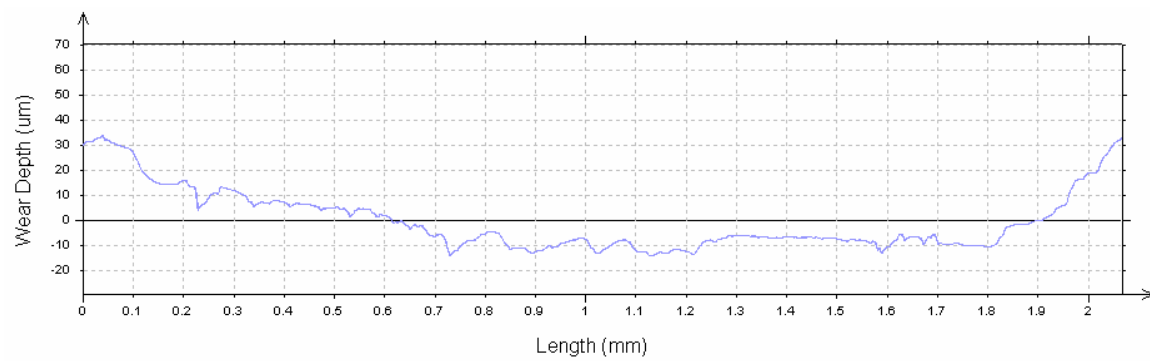


Figure 3.5 Typical Fretting Scar (Test 5)



**Figure 3.6 Profilemeter Measurement of Surface (Test 1)**



**Figure 3.7 Profilemeter Measurement of Surface (Test 7)**

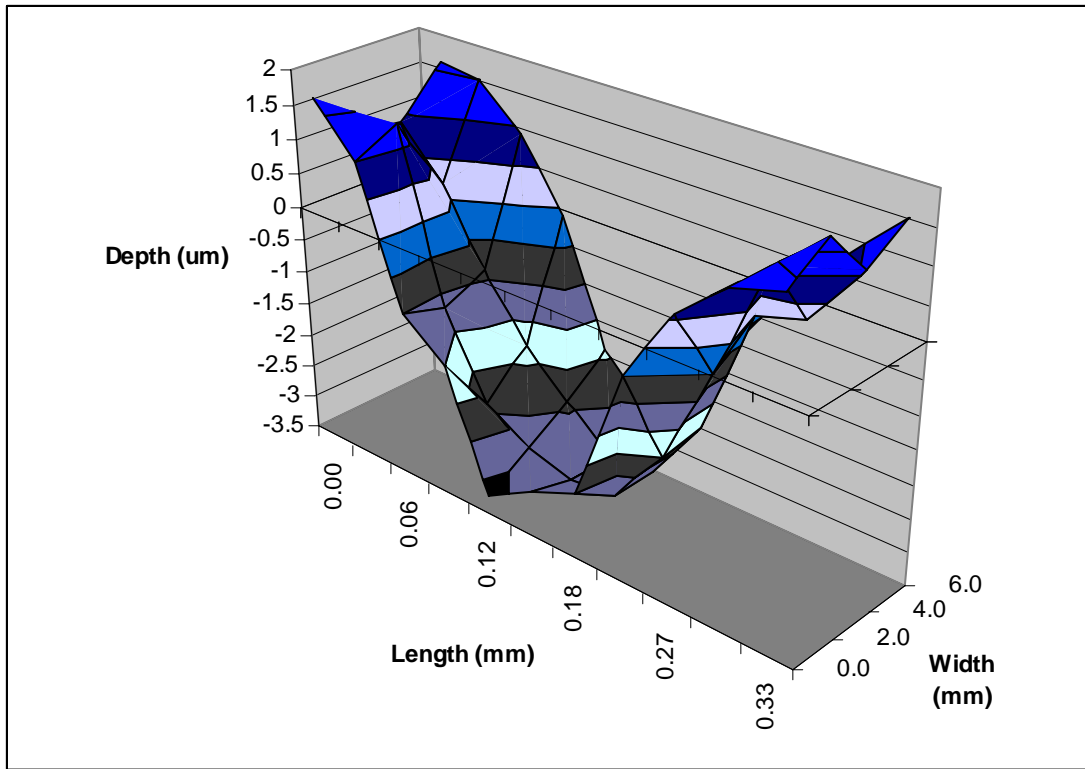


**Figure 3.8 Three-Dimensional Surface Profile (Test 1)**

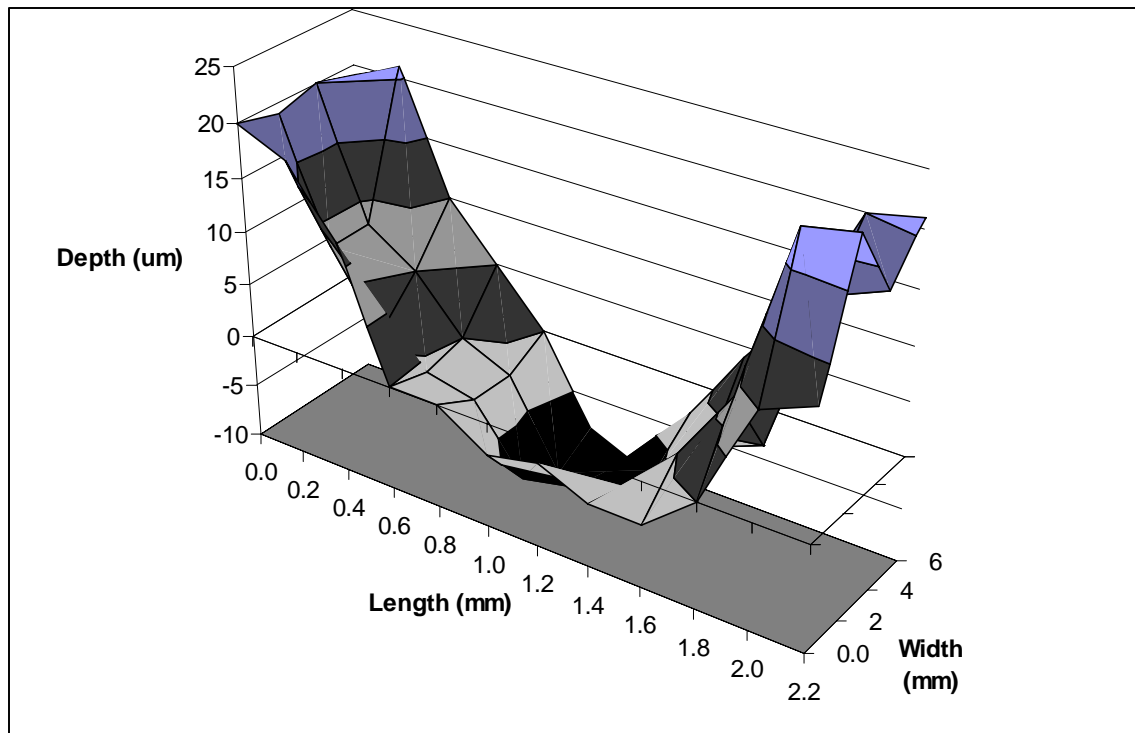


**Figure 3.9 Three-Dimensional Surface Profile (Test 7)**

**Table 3.1 Program of Experimental Tests**

Test #	Fatigue Load	Applied Dis. ( $\mu\text{m}$ )
1	N	75
2	N	150
3	N	300
4	N	600
5	Y	0
6	Y	300
7	Y	450

## IV. Results and Discussion

As the fretting tests were being run, data were recorded via the *MTS* software. The data of importance that were recorded were the load measurement from the lower actuator, load measurement from the upper frame, load measurement from the upper actuator, the displacement of the lower and upper actuators, and the strain of the extensometer (used to determine displacement length). The data were recorded at a sampling rate allowing 20 measurements per cycle. A summary of the data from the experimental testing of this current study can be seen in Table 4.1. As can be seen by comparing the data from this study with that of Lee's previous study [12] in Table 4.2, the applied displacements used in both studies did not result in the same relative displacements and tangential forces. The effect of fatigue load in tests 4-7 of the current study was an additional increase in the relative displacement for these tests. The same applied displacements for tests with no fatigue resulted in much lower relative displacements than those tests that had a fatigue load.

### 4.1 Fretting Loops:

Fretting loops are a plot of tangential force,  $Q$ , verses relative displacement,  $\delta$ , plotted for each cycle of a fretting test. An analysis of the fretting loops can give a great deal of information about the wear process. One of the main characteristics that can be defined by analysis of the fretting loops is the fretting regime, i.e., type of slip that was taking place during the test.

#### 4.1.1 Fretting Regime:

The fretting regime was determined from analysis of the fretting loop for each test. Partial slip is characterized by thin, elliptical shape loops. Figure 4.1 shows the fretting loops for a test that was of the partial slip regime, and, as can be seen, partial slip was occurring by the 100<sup>th</sup> cycle and continued until the end of the test. Gross slip is characterized by quasi-rectangular loops that stay relatively constant in size through the testing period; an example of gross slip can be seen in Figure 4.2. A third type of slip regime present in the current study was that of mixed-mode, though it was not present in any of the tests in the Lee study [12]. A mixed-mode slip regime resembles that of gross slip, but, at some point, the loops start to change from quasi-rectangular and become slightly more elliptical in shape (see Figure 4.3). A characteristic of the mixed-mode regime is that the loops do not become as elliptical as they do with partial slip and the area inside the fretting loop is much larger than that under partial-slip conditions. If the fretting tests were allowed to carry on substantially longer for the mixed-mode regime tests, it is believed that the fretting regime would eventually change to partial slip at some point, as was found in the Jin study [8].

A comparison was made between the fretting loops of the tests conducted without a fatigue load and tests conducted with a fatigue load. The fretting loops generated at the end of testing (at the 15,000<sup>th</sup> cycle) can be seen for each test in Figure 4.4 and Figure 4.5. Partial slip only occurred for tests with no fatigue load. The areas inside the loops for the tests conducted with fatigue are much larger—the effect of the fatigue load essentially caused much greater displacements to occur.

## 4.2 Wear Analysis:

The wear analyses of the fretting tests in this study were conducted in such a way that data from one study could be compared with data from another study. Several methods have been used by previous researchers to characterize wear for similar fretting tests. The two principal methods used by Lee [12] and that were also used in this study were the accumulated relative displacement method and accumulated dissipated energy method. Wear depth and tangential force were also analyzed.

### 4.2.1 Accumulated Relative Displacement Method:

The accumulated relative displacement method used by Lee [12] is similar to the Archard model used to quantify the wear evolution of fretting under gross conditions [1]. With this method, the wear volume is compared with the accumulated relative displacement range (see Figure 4.6). One of the benefits of the accumulated relative displacement method is that the data are calculated more easily than when using other methods. The accumulated relative displacement range ( $\Delta\delta_c$ ) was calculated by summing the relative displacement range from each cycle ( $\Delta\delta_i$ ) over the total number of cycles in a fretting test (N), such that:

$$\Delta\delta_c = \sum_{i=1}^N \Delta\delta_i \quad (11)$$

where

$$\Delta\delta_i = \delta_{\max} - \delta_{\min}, \text{ for each cycle} \quad (12)$$

As can be seen in Figure 4.6, the relationship between wear volume and accumulated relative displacement is linear for all of the slip regimes and loading

conditions studied in both this study and that of Lee [12]. For a similar amount of accumulated displacement, the wear volumes measured for the tests conducted in the current study are much less than those measured in the Lee study. Wear is proportional not only to the contact load and relative displacement, but also to the surface conditions, and, thus, a change in the CoF at the contact surface will result in a change in the amount of wear. Unfortunately, tests conducted with greater wear volumes were unable to be conducted due to the limited range of the extensometer, so data on the higher end of the curve for the Lee study could not be compared in this study.

#### 4.2.2 Accumulated Dissipated Energy Method:

Though the accumulated relative displacement method does show a linear trend for the data, previous studies have found that similar methods do not incorporate the friction coefficient in their description [2-4]. The purpose of this study is to analyze the effect that a change in CoF has on the wear of the Cu-Al coating, so it is important to use a method that incorporates the friction coefficient. To include the CoF, the wear volume can be compared with the accumulated energy dissipated through the interface between the pad and specimen [3].

The total accumulated dissipated energy ( $E_c$ ) in a fretting test can be obtained by summing the dissipated energy from each cycle ( $E_i$ ) over the total number of cycles (N), such that:

$$E_c = \sum_{i=1}^N E_i \quad (13)$$

The dissipated energy for each cycle ( $E_i$ ) was equal to the area inside the fretting loop. To calculate the area inside the fretting loop, a higher-order polynomial fit was created for both the upper and lower curves with advanced mathematical software (*Mat Lab*). With a polynomial approximation that closely fit the curves known, it was possible to integrate the area under the upper and lower curves. The area of the lower curve was then subtracted from the area of the upper curve to calculate the area inside the fretting loop and, thus, the dissipated energy for each cycle.

Plots of wear volume verses accumulated dissipated energy for the tests conducted in this study and those of Lee [12] can be seen in Figure 4.7 and Figure 4.8—the relationship between wear volume and accumulated dissipated energy is also a linear one. It was expected that, due to a decrease in the CoF, the wear volume for a similar amount of dissipated energy would be less for tests conducted in this study, compared with those of Lee. Actual analysis shows that there is not much difference—the wear volume for tests conducted in this study are actually slightly higher for a similar amount of dissipated energy. This is most likely due to the ambiguity of the wear-volume measurements. Due to the relatively rough coating surface, it was sometimes difficult to accurately measure the wear areas from the surface profiles and thus determine a reliable wear volume for each test.

A linear regression line was calculated for the data of the Lee study and the current study, and, from this, the energy wear coefficient was determined. The energy wear coefficient is the slope of the regression line; for the Lee study it was about 2.85E-04 mm<sup>3</sup>/J, and for the current study testing it was about 4.03E-4 mm<sup>3</sup>/J.

In a previous study [3] that conducted fretting tests in a similar manner, there was a shift in the linear relationship from the origin on the energy axis. In fretting tests, it is possible that, during the incipient loading, the surface endures severe strain-hardening, which modifies the initial microstructure to a very hard phase called a tribologically transformed structure (TTS). When this TTS layer is formed, wear cannot occur until the TTS layer is fractured; this phenomenon can account for the shift on the energy axis. As found in Lee's results [12], the linear relationship in this study started very close to the origin on the energy axis. The y-intercept value determined from the regression line was only  $0.015 \text{ mm}^3$ —a very minor shift; this signifies that a TTS layer was never formed during the testing in the current study.

#### 4.2.2.1 Normalized Wear Depth:

The normalized wear depth as a function of the accumulated dissipated energy was also analyzed to further compare data from this study with those of Lee [12], and the depth can be seen in Figure 4.9. The normalized wear depth was calculated for each test as the ratio of the maximum wear depth to the initial thickness of the coating, which, in this study, was  $40 \mu\text{m}$ .

As occurred when comparing wear volume to accumulated dissipated energy between the two studies, there were minor differences when comparing normalized wear depth, again most likely due to ambiguity in reading the surface profile measurements. In the Lee study, tests were conducted in which all of the coating was worn away and the normalized wear depth was 1.0 or greater. In the current study, there was a linear increase in wear depth with energy, but the normalized wear depth was never greater than

0.4 and the coating was never worn away—despite the large displacements that were applied in the current study.

#### 4.2.2.2 Tangential Force:

The energy method takes into account both relative displacement and tangential force, and the results from analyzing the data from the two different studies with this method were similar. However, for a similar amount of wear volume, the relative displacements for the tests of this study were much greater than those of the previous study, so the tangential forces must be different as well. The differences in tangential force were then analyzed to help further characterize the fretting wear and contact conditions. Plots of tangential force ( $Q_{\max} - Q_{\min}$ , i.e.,  $\Delta Q$ ) for each cycle can be seen in Figure 4.10.

The tangential forces measured in this study were significantly lower than those measured by Lee. Previous studies [18] have researched the relationship between the generation of wear debris and tangential force. An increase in the amount of wear debris participating in the friction process has been found to consequently result in an increase in the tangential force. Because the lubricant was entering the contact region and possibly helping to remove some of the wear debris, and because the CoF in the current study was lower than that of Lee, it was expected that the tangential force for the test cycles of the current study would be significantly lower.

In the Lee study, most of the tests showed an increase in tangential force with an increase in the amount of fretting cycles. The tangential force in the Lee study leveled off at a value approximately equal to the applied contact load. In the current study, the

tangential force stayed relatively constant, increased, or increased and then decreased. The tangential force in the current study never increased and then leveled off, as in Lee's study—this was because the tangential force never came close to reaching the applied contact load value. In this study, tests conducted under lower energy conditions had a tangential force that stayed mostly constant, as in Test 1, in which the contact condition was one of partial slip. Tests with higher energy conditions did show an increase in tangential force as the testing cycles went on became similar to those that occurred in the Lee study. There were two tests in which the tangential force actually decreased during the later part of cycling, which was not observed by Lee.

As can be seen in Figure 4.10, there is some decrease in the tangential force in the later part of the testing cycles for Tests 5 and 7; there are several possible reasons for this result. During the fretting tests, as the contact surfaces were worn due to material loss, the compressive springs that applied the normal contact load to the fretting pads were able to expand slightly and no longer provided the same initial contact force of 320 N—this was also observed by Magaziner [14]. Magaziner attributed this effect to the oscillations in  $Q$ , as plotted against  $N$ , and the reduction of the tangential force in value during the later part of cycling. This oscillation and reduction in tangential force were also observed in the current study for tests that resulted in high wear volumes (Tests 5 and 7), but not in all tests (Test 6), so this may not be a viable explanation for what occurred. In the Jin study [8], it was found that, for tests in the mixed-mode regime, there was some increase and decrease in  $Q$ —some variation of the tangential force with increasing fretting fatigue cycles. This characteristic of mix-mode contact conditions could explain the variation and decrease in tangential force for Tests 5 and 7. Analysis

and testing of this needs to be researched further to determine why mixed-mode occurred for Test 5 and 7 whereas only gross slip occurred for Test 6.

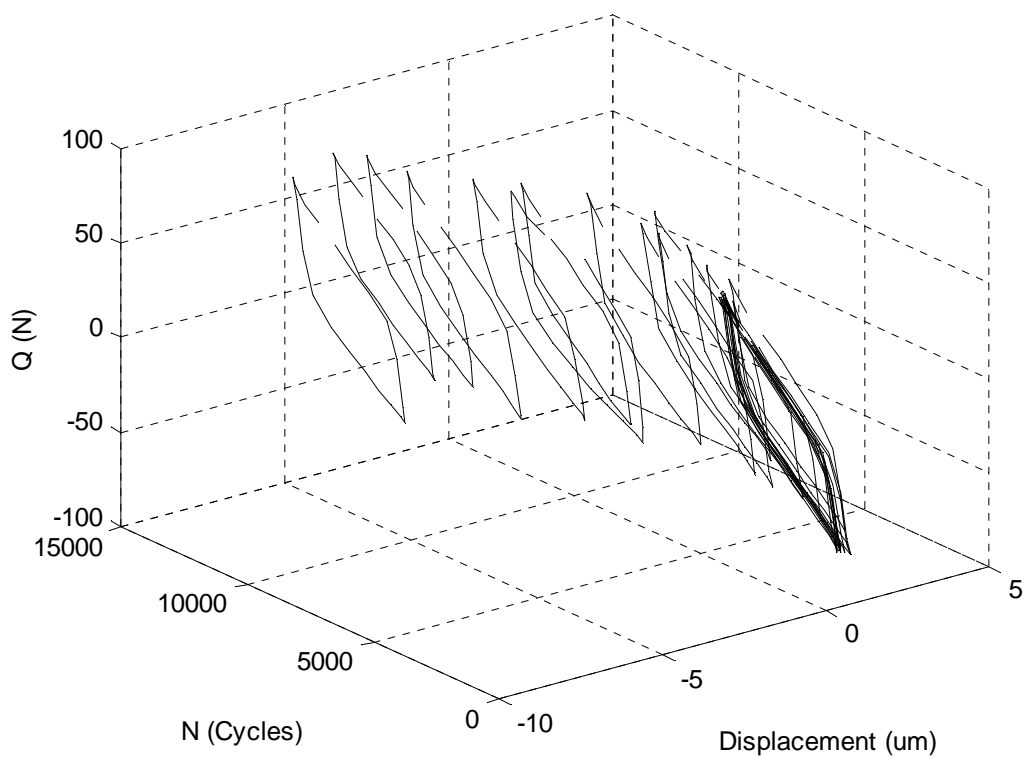


**Figure 4.1 Typical Fretting Loops of Partial Slip (Test 1)**

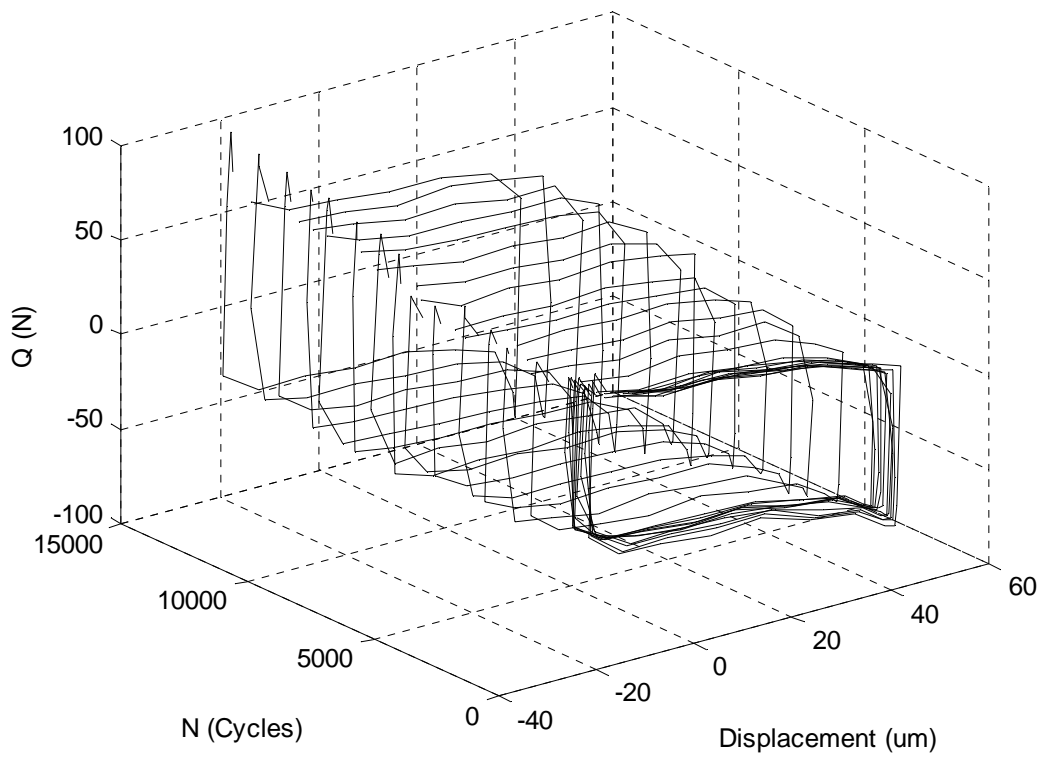


**Figure 4.2 Typical Fretting Loops of Gross Slip (Test 4)**

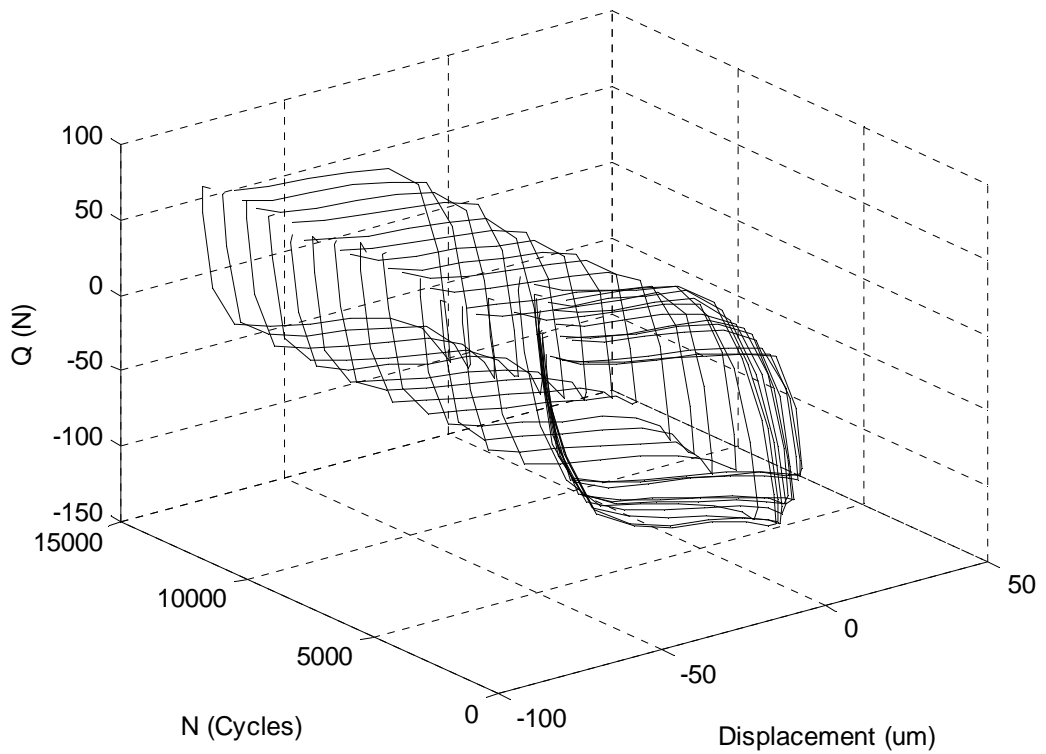


**Figure 4.3 Typical Fretting Loops of Mixed-Mode (Test 5)**

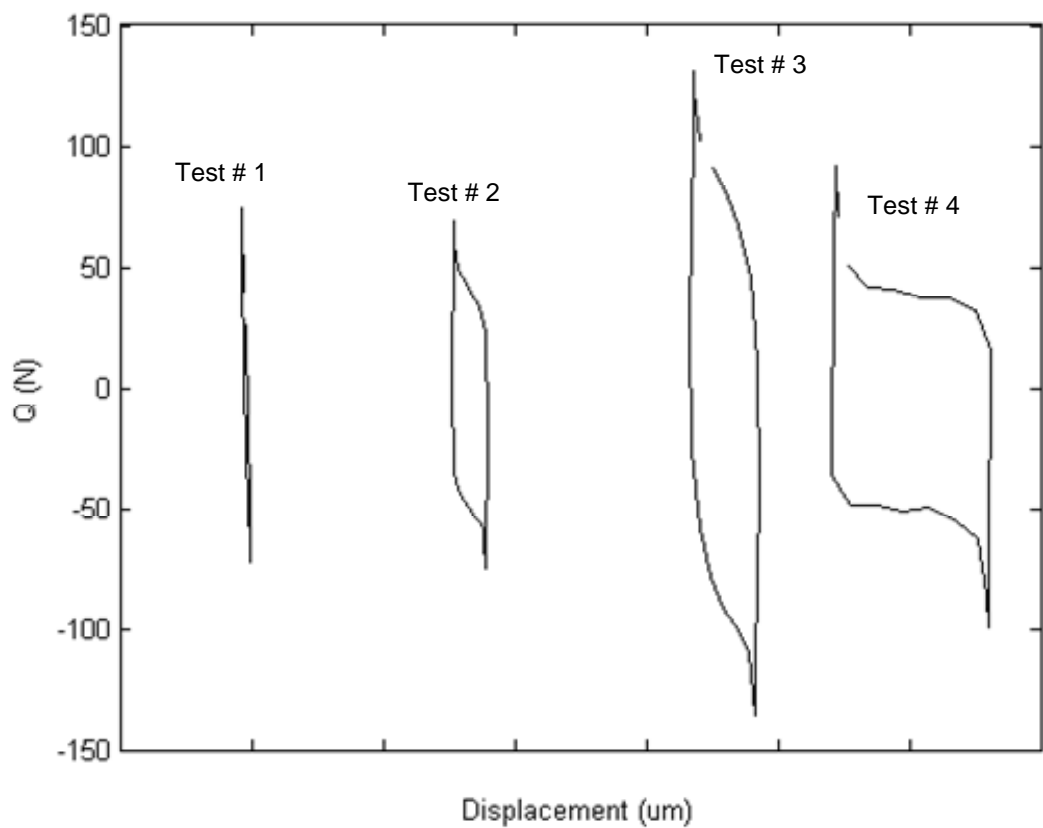


**Figure 4.4 Fretting Loops at the 15,000<sup>th</sup> Cycle for Each Test (No Fatigue)**

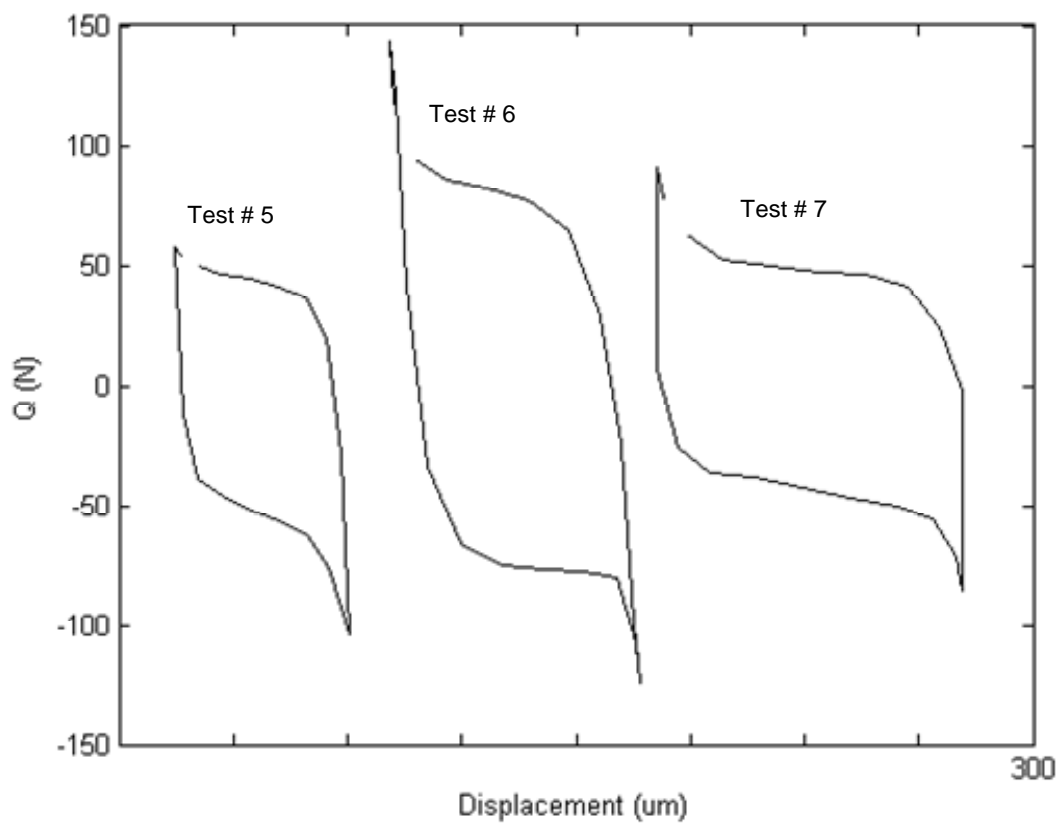


**Figure 4.5 Fretting Loops at the 15,000<sup>th</sup> Cycle for Each Test (Fatigue)**

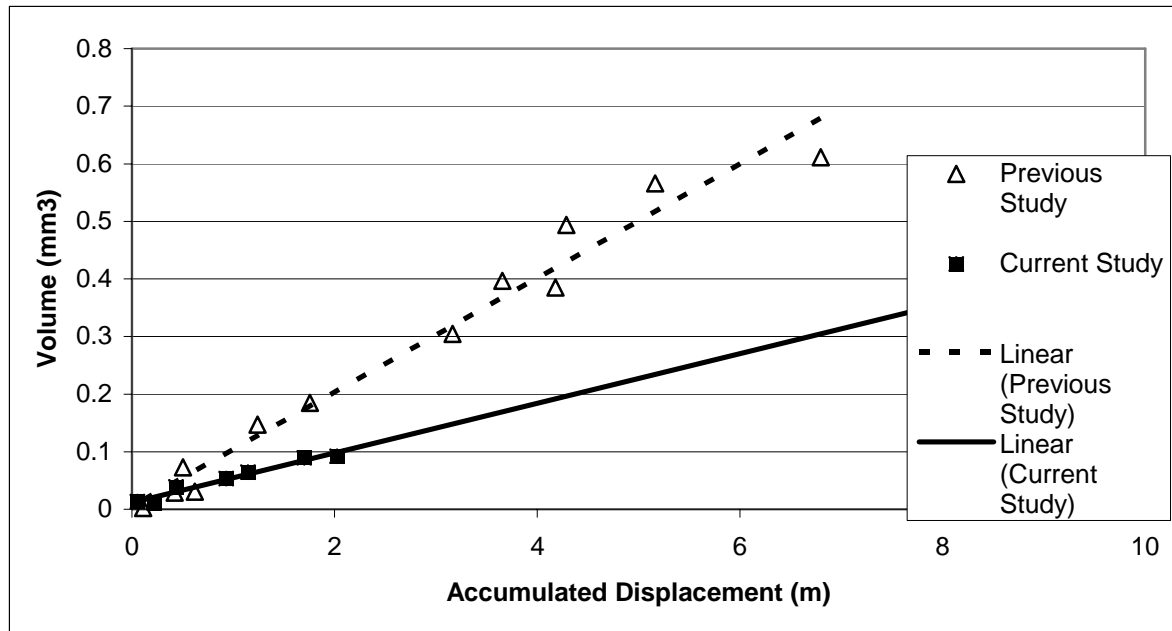


**Figure 4.6 Accumulated Relative Displacement Range vs. Wear Volume**

(Note: previous study data from Lee [12])

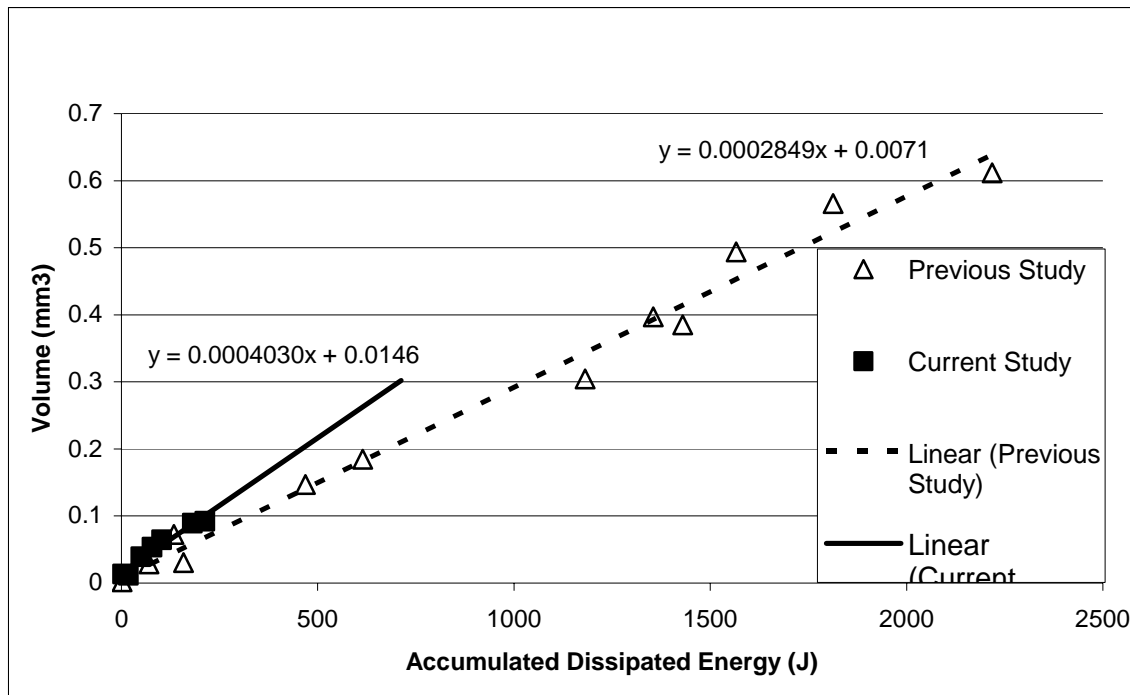


**Figure 4.7 Accumulated Dissipated Energy vs. Wear Volume**

(Note: previous study data from Lee [12])

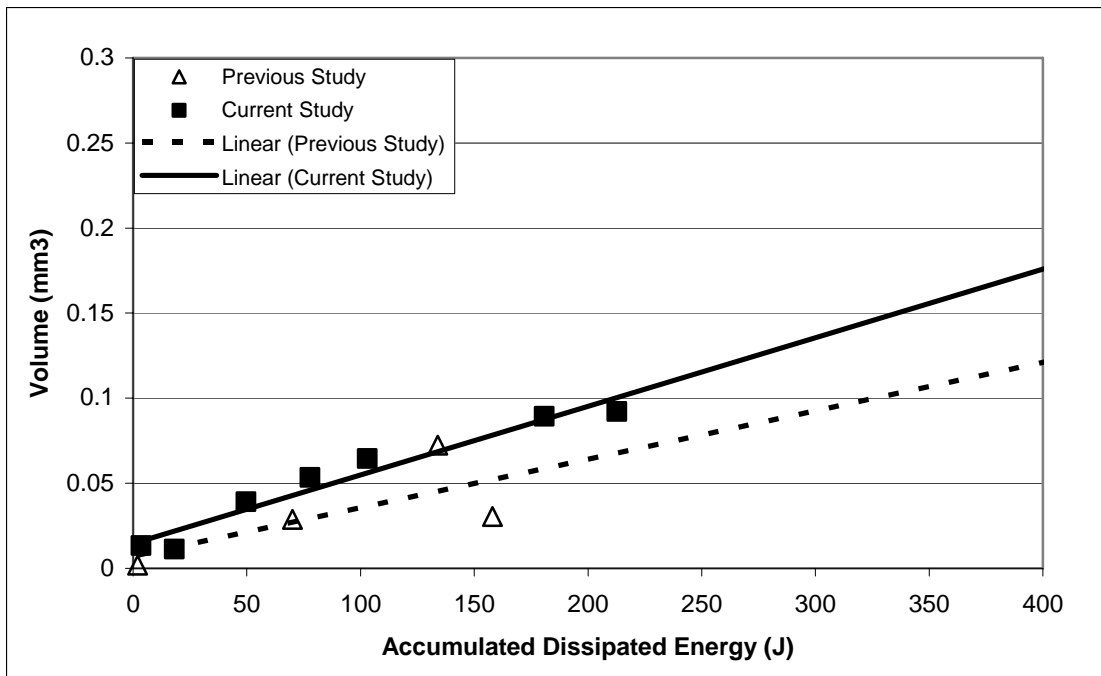


**Figure 4.8 Close-in View of Accumulated Energy for Current Study**

(Note: previous study data from Lee [12])

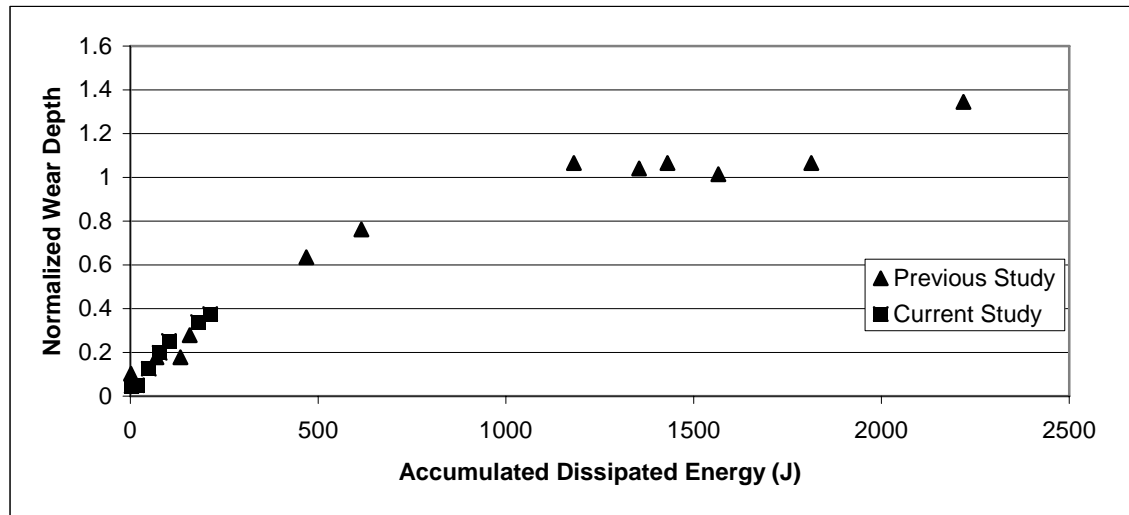


**Figure 4.9 Normalized Wear Depth vs. Accumulated Dissipated Energy**

(Note: previous study data from Lee [12])

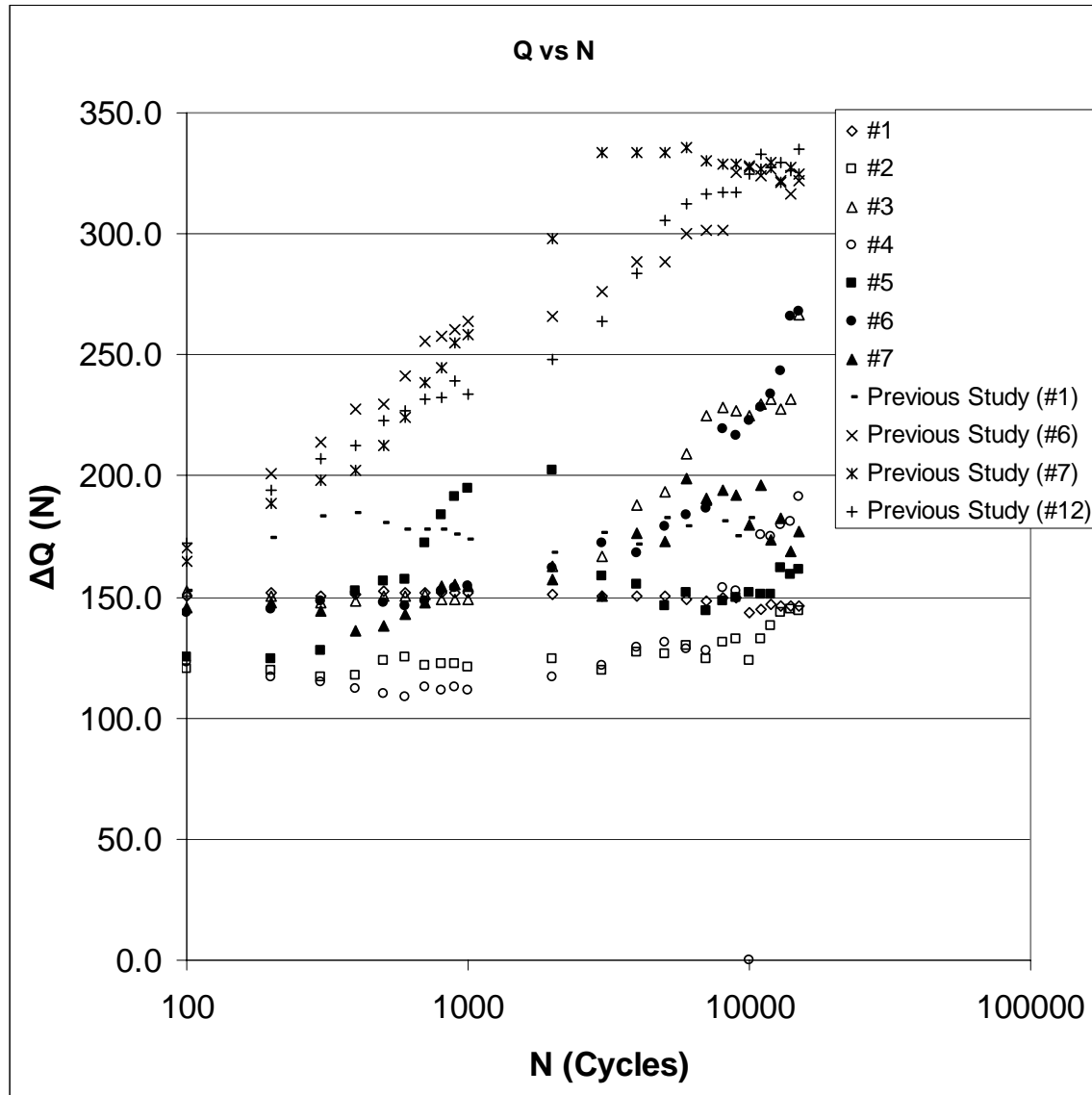


**Figure 4.10 Tangential Force vs. Number of Cycles**

(Note: previous study data from Lee [12])

**Table 4.1 Data Summary for Current Study**

Test #	Fatigue Load	Applied Dis.	$\Delta$ Realt. Dis	Q	Fretting Regime
		( $\mu\text{m}$ )	( $\mu\text{m}$ )	(N)	
1	N	75	3.1	147	Partial
2	N	150	14	144	Partial
3	N	300	27	266	Gross
4	N	600	61	191	Gross
5	Y	0	76	161	Mixed
6	Y	300	109	268	Gross
7	Y	450	134	177	Mixed

(Note: Q value given is  $\Delta Q$  for 15,000<sup>th</sup> cycle)**Table 4.2 Data Summary for Lee Study [12]**

Test #	Fatigue Load	Applied Dis.	$\Delta$ Realt. Dis	Q	Fretting Regime
		( $\mu\text{m}$ )	( $\mu\text{m}$ )	(N)	
1	N	150	6	182	Partial
2	N	300	17	300	Partial
3	N	430	59	304	Gross
4	N	480	212	297	Gross
5	N	530	272	294	Gross
6	N	630	450	310	Gross
7	Y	0	20	282	Partial
8	Y	50	30	323	Partial
9	Y	130	50	362	Gross
10	Y	150	170	323	Gross
11	Y	280	288	325	Gross
12	Y	380	330	336	Gross

(Note: Q value given is  $\Delta Q$  for 15,000<sup>th</sup> cycle)

## V. Conclusions

### 5.1 Summary of Problem:

Fretting fatigue has plagued and continues to be an issue for both the designers and the maintainers of jet turbine engines of aircrafts in our nation's air forces. Designers must "over-design" the turbine blades, making them larger and less efficient to account for fretting fatigue. Maintenance workers must spend valuable time, at a significant cost to the government, inspecting turbine blades for possible cracks caused by fretting fatigue. Titanium is the material commonly used to construct turbine blades, and there have been numerous studies aimed at researching possible ways to eliminate or decrease the fretting fatigue of titanium. Previous studies have found that Cu-Al coating applied to Ti-6Al-4V may help to decrease fretting fatigue. Though soft Cu-Al coating may help to reduce fretting fatigue, hard microhardness is required to resist abrasion wear mechanism—as a result, the Cu-Al coating is susceptible to significant abrasion wear. The goal of this study was to analyze the effect of a change in the CoF at the contact region in fretting wear of a Cu-Al coating applied to a titanium substrate.

### 5.2 Summary of Results:

Tests conducted with a lower CoF value at the contact surface had considerably different wear characteristics, as compared with the tests conducted with a higher CoF value. One major difference was that, for experimental tests conducted in this study, a much larger amount of displacement had to be applied to achieve similar relative

displacement values, compared with the displacement used in the previous study [12]—even though the same fretting-test setup was used.

When the wear of the coating was analyzed with the accumulated relative displacement method, there were differences between the tests conducted with different CoF values, though both studies displayed similar linear trends when scrutinized from the point-of-view of this method. This method, however, did not account for the frictional force effects in the analysis

A more useful method for analyzing the data was with the accumulated dissipated energy method. This method took into account both the relative displacement and the tangential force that is obviously affected by changes in the CoF. By lowering the CoF, both the relative displacement and tangential force were affected, which resulted in similar wear characteristics when analyzed with the accumulated dissipated energy method.

### 5.3 Knowledge Gained from Study:

The main purpose of this study was to analyze the wear of the Cu-Al coating applied to a Ti-6Al-4V substrate and the effect that a change in CoF can have on it. By decreasing the CoF, the coating wear was also decreased, which thus relates to an increase in coating life. It has already been shown in previous studies [17, 16, 11] that an increase in coating life can be very beneficial in decreasing fretting damage. The tangential forces also decreased due to the use of a liquid lubricant and, thus, lower CoF,

which means that shear stresses placed on the specimen will be much lower. This decrease in the shear stresses is also advantageous in reducing fretting fatigue damage.

## VI. Future Work

There is a great deal of work that remains to be undertaken not only in the general study of fretting fatigue, but also in regards to the specifics covered in this study. An understanding of the wear of Cu-Al coating under fretting conditions has only begun to be developed and much more work could be performed on a number of different variables, including the CoF effects, which were analyzed in this study.

### 6.1 Tests with Longer Extensometer Gauge Length:

In the Lee study [12], a 0.5-in. extensometer was used, whereas, in this study, a 0.3-in. extensometer was used. The use of the smaller gauge length extensometer did allow more accurate measurements to be conducted with less uncertainty, which was a benefit, but there were also disadvantages of using the 0.3-in. model as well. The smaller gauge length meant that the extensometer also had a smaller range of motion. The displacement that could be applied while conducting the tests was limited to prevent the extensometer from being stretched out to its maximum range.

For future work, an extensometer with a gauge length even larger than 0.5 in. could be used so that tests could be conducted with a much greater displacement than were performed in this study with the smaller extensometer. This would allow tests to be run to reach higher wear volumes, accumulated displacement, and accumulated energy data values. Currently, data from this study only fall on the lower end of the spectrum, as compared with Lee's results [12]. It is difficult to make a comparison between the data from this study and the data from Lee's studies for the tests run with much higher wear

volume, accumulated displacement and accumulated energy. Though tests conducted with a larger extensometer would be less accurate, they would allow the curves in

and Figure 4.7 to be pushed further to the right and up for a better comparison between the dry and lubricated conditions at higher wear volumes.

For tests run with higher applied displacements and, thus, most likely greater tangential forces, it would also be possible to examine how high the tangential forces can become. With the possibility of inducing greater tangential forces, observation could also be made to determine if the tangential forces reach an equilibrium level approximately equal to the contact load, as occurred in the previous Lee study [12].

### 6.2 Data Points Recorded per Cycle:

The fretting loops created and analyzed in this study were fairly choppy and uneven compared with the fretting loops created in other studies. Based on initial trial experimentation, it was determined that a data-collection rate of 20 points per cycle would be sufficient; it is now realized that a higher sampling rate would probably have been more beneficial and would have resulted in more even fretting loops. More even fretting loops with more data points would also have allowed more accurate curves to be fitted to the data when calculating the area in the fretting loops for accumulated dissipated energy analysis.

### 6.3 SEM Analysis:

Future work that could also be performed is analysis of the fretting scars with a Scanning-Electron-Microscope (SEM). Previous studies such as Jin [10] have found

success in further characterizing the contact conditions and in examining the nature of the damage in the contact area by looking at SEM images of the fretting scars. SEM images could be used to help explain why there was a decrease in tangential force in the later part of cycling for Tests 5 and 7 but not Test 6 by analyzing their fretting scars and debris buildup.

## **Appendices**

### **A1 Sample Data:**

A sample spreadsheet of the data recorded has been included to help guide future researchers following this work.

**Table A1.1 Example of Raw Data Measurements (Test 4)**

Cyclic Acquisition			Test #5_600 dis_no fat(10APR)						Time:	65.05 Sec											
Stored $\alpha$	100 cycle		Stored for:			2 segments			Calculated Values												
Points:	20																				
Time	upper	Upper	Forc	upper	Upper	Displ	lower	Displ	lower	frame	cell	lower	Act cell	Strain							
Sec	N		mm		mm	N		N		N	mm		um	um	um	um	Delta A	Delta DC	Delta ext	Delta (x)	Q (z)
54.274	115.85796		35.273251		-30.51522	-725.93225		-635.30927		-0.027033			-8.93	-0.48791	-27.0331	-17.6151	45.3115				
54.299	119.08804		35.298283		-30.51888	-737.00342		-625.36224		-0.029521			-9.066	-0.601071	-29.5211	-19.8537	55.8206				
54.324	101.74963		35.29985		-30.51895	-722.32843		-645.9248		-0.029636			-8.886	-0.411353	-29.6362	-20.3391	38.2018				
54.349	-63.479603		35.285038		-30.52088	-647.38281		-707.08954		-0.028758			-7.964	0.321458	-28.7582	-21.1159	-29.8534				
54.374	-65.328377		35.218666		-30.51666	-634.00964		-718.20959		-0.022352			-7.799	0.453328	-22.3518	-15.0059	-42.1				
54.399	-85.202507		35.132164		-30.51708	-629.10199		-714.77002		-0.013655			-7.739	0.461232	-13.6554	-6.37776	-42.834				
54.424	-68.307617		35.029839		-30.51966	-625.19269		-717.39233		-0.003618			-7.691	0.496398	-3.61761	3.576818	-46.0998				
54.448	-87.047096		34.927395		-30.51761	-622.60724		-710.88269		0.0065384			-7.659	0.475271	6.538405	13.72216	-44.1377				
54.473	-84.849144		34.827053		-30.51757	-615.20398		-719.6153		0.0169078			-7.568	0.562145	16.90776	23.91357	-52.2057				
54.498	-108.05887		34.735325		-30.51534	-606.9397		-718.33514		0.0263086			-7.466	0.599747	26.30864	33.17518	-55.6977				
54.523	-108.04141		34.673061		-30.51473	-595.61163		-726.45715		0.0324372			-7.327	0.704466	32.43724	39.05971	-65.4228				
54.548	-132.31406		34.651058		-30.51646	-590.21063		-724.40631		0.0346413			-7.26	0.722503	34.64127	41.17926	-67.0978				
54.573	-92.158684		34.65181		-30.52069	-600.68719		-714.41058		0.034959			-7.389	0.612281	34.95898	41.73607	-56.8617				
54.598	48.334476		34.669296		-30.51576	-676.20557		-642.41693		0.0338646			-8.318	-0.181916	33.86464	42.36492	16.8943				
54.623	75.562302		34.729549		-30.5192	-685.5614		-642.03546		0.0279509			-8.433	-0.234341	27.95091	36.61871	21.763				
54.648	67.858719		34.826729		-30.51782	-693.61145		-636.74207		0.0185378			-8.532	-0.306182	18.53776	27.37642	28.4347				
54.673	93.93779		34.919762		-30.51896	-702.63141		-637.05255		0.0091338			-8.643	-0.353073	9.133814	18.13033	32.7894				
54.698	84.369568		35.019531		-30.52139	-707.04102		-634.51587		-0.001062			-8.698	-0.390472	-1.06211	8.026051	36.2626				
54.722	100.7383		35.115223		-30.51552	-710.83655		-638.38116		-0.010811			-8.744	-0.390096	-10.8114	-1.67692	36.2277				
54.747	89.644417		35.20845		-30.5208	-715.73792		-635.1557		-0.020616			-8.805	-0.433851	-20.6159	-11.3774	40.2911				
Cyclic Acquisition			Test #5_600 dis_no fat(10APR)						Time:	105 Sec											
Stored $\alpha$	200 cycle		Stored for:			2 segments			Calculated Values												
Points:	20																				
Time	upper	Upper	Forc	upper	Upper	Displ	lower	Displ	lower	frame	cell	lower	Act cell	Strain							
Sec	N		mm		mm	N		N		N	mm		um	um	um	um	Delta A	Delta DC	Delta ext	Delta (x)	Q (z)
104.28	116.27216		35.279144		-30.51946	-725.10437		-640.26587		-0.027441			-8.92	-0.456766	-27.4414	-18.0647	42.4193				
104.3	113.78419		35.29966		-30.51612	-736.66455		-633.25751		-0.029552			-9.062	-0.556738	-29.5518	-19.9329	51.7035				
104.33	78.188141		35.295837		-30.5156	-709.56531		-659.19061		-0.029501			-8.729	-0.271215	-29.5011	-20.5011	25.1874				
104.35	-57.593925		35.272923		-30.51388	-651.78406		-711.33447		-0.02777			-8.018	0.320616	-27.7698	-20.0725	-29.7752				
104.38	-60.908611		35.20322		-30.51548	-635.44031		-720.99152		-0.020855			-7.817	0.460603	-20.8554	-13.4991	-42.7756				
104.4	-83.697136		35.11536		-30.5172	-633.23248		-717.02283		-0.012098			-7.79	0.451123	-12.0976	-4.75898	-41.8952				
104.43	-66.791718		35.015041		-30.51751	-628.12122		-716.4082		-0.001985			-7.727	0.475333	-1.98454	5.266975	-44.1435				
104.45	-85.813408		34.917412		-30.51389	-627.30029		-714.34131		0.0080871			-7.717	0.468624	8.087056	15.33518	-43.5205				
104.48	-81.782555		34.812908		-30.51545	-616.91663		-721.43195		0.018329			-7.589	0.562705	18.32902	25.35534	-52.2577				
104.5	-109.63203		34.726192		-30.51749	-611.03986		-722.30585		0.0272602			-7.517	0.599051	27.26024	34.17791	-55.633				
104.53	-108.01971		34.673244		-30.51615	-599.55908		-726.45776		0.032669			-7.375	0.683216	32.669	39.36128	-63.4493				
104.55	-128.09908		34.653652		-30.51674	-595.57416		-725.66638		0.0345722			-7.326	0.70041	34.5722	41.19826	-65.0461				
104.58	-61.676838		34.65591		-30.51249	-617.75098		-703.3255		0.034675			-7.599	0.460729	34.67504	41.81359	-42.7873				
104.6	35.456059		34.680187		-30.5142	-678.48529		-649.03168		0.0326552			-8.346	-0.158577	32.65519	41.16017	14.7268				
104.63	76.597794		34.747833		-30.5138	-685.87909		-646.81458		0.026304			-8.437	-0.210321	26.30404	34.95172	19.5323				
104.65	64.614212		34.843052		-30.51594	-696.75116		-640.60284		0.0169216			-8.571	-0.3023	16.92158	25.79498	28.0742				
104.68	91.222839		34.935955		-30.51539	-702.98822		-642.26703		0.0076327			-8.648	-0.32692	7.632744	16.60749	30.3606				
104.7	78.581879		35.034676		-30.51589	-709.53107		-639.22498		-0.002548			-8.728	-0.378524	-2.54783	6.559013	35.153				
104.73	97.5112		35.12825		-30.51562	-710.7066		-643.26123		-0.012187			-8.743	-0.363122	-12.1866	-3.0807	33.7227				
104.75	87.202682		35.222313		-30.51732	-719.53918		-638.64722		-0.021726			-8.851	-0.435518	-21.7256	-12.4387	40.446				

## A2 CoF Force Measurements:

The CoF calculated in this experiment for the wet condition was  $\sim 0.13$ , and for the dry condition was determined to be  $\sim 0.24$ , whereas, in the Lee study, it was  $\sim 0.20$ . This is a difference that can be accounted for in slight variations in which the measurements were conducted; the important note is the difference between the CoF values measured for the wet and dry conditions in this study. The data used to make the CoF calculations have been included in the case that future researchers also measure CoF—with this they can compare their data with those of the current study.

**Table A2.2 CoF Measurement Data**

Condition	Force Reading #1 (N)	Force Reading #2 (N)	Force Reading #3 (N)	Note: P=320 N
Dry	72	80	74	Average = 75.3
				CoF = 0.24
Wet	42	47	32	Average = 40.3
				CoF = 0.13

### A3 Tests with Greater Wear Volumes:

Tests were conducted with a higher level of applied displacement both with and without fatigue that resulted in a complete wear of the coating and much greater wear volumes (see Figure A3.1 and Table A3.1). Unfortunately, the 0.3-in. extensometer was pushed to its maximum range for these tests and did not record the relative displacement accurately, so these tests could not be included in analysis. Use of an extensometer with a larger gauge length would have eliminated this problem.



**Figure A3.1 Scar with Complete Coating Wear (Test #8)**

**Table A3.1 Extra Tests with Complete Coating Wear**

Test #	Fatigue Load	Applied Dis. (μm)	Wear Volume (mm <sup>3</sup> )
8	N	825	0.0000
9	Y	600	0.0000

## Bibliography

1. Archard, J.F. *Journal of Applied Physics*. 1953; 24: 981.
2. Fouvry, S., and P. Kapsa. "An Energy Description of Hard Coating Wear Mechanisms." *Surface and Coatings Technology*. 2001; 138: 141-148.
3. Fouvry, S., P. Kapsa, and L. Vincent. "An Elastic-plastic Shakedown Analysis of Fretting Wear." *Wear*. 2001; 247: 41-54.
4. Fouvry, S., T. Liskiewicz, P. Kapsa, S. Hannel, and E. Sauger. "An Energy Description of Wear Mechanisms and its Applications to Oscillating Sliding Contacts." *Wear*. 2003; 255: 287-298.
5. Gabel, M., and J. Bethk. "Coatings for Fretting Prevention." *Wear*. 1979; 46: 81-96.
6. H. Hertz, "Uber die Berugrung fester elastischer Korper," *J. Reine Angew. Math.*, 92 (1882) 156-171.
7. Hills, D., D. Nowell, and A. Sackfield. *Mechanics of Elastic Contacts*. Oxford: Butterworth-Heinemann Ltd., 1993.
8. Jin, O., and S. Mall. "Effects of Independent Pad Displacement on Fretting Fatigue Behavior of Ti-6Al-4V." *Wear*. 2002; 253: 585-596.
9. Jin, O., and S. Mall. "Effects of Slip on Fretting Behavior: Experiments and Analyses." *Wear*. 2004; 256: 671-684.
10. Jin, O., S. Mall, J.H. Sanders, and S.K. Sharma. "Durability of Cu-Al Coating on Ti-6Al-4V under Fretting Fatigue." *Surface and Coatings Technology*. April, 2006.
11. Jin, O., S. Mall, J.H. Sanders, and S.K. Sharma. "Fretting Fatigue Behavior of Cu-Al Coated Ti-6Al-4V."
12. Lee, H., S. Mall, J. Sanders, and S.K. Sharma. "Wear Analysis of Cu-Al Coating on Ti-6Al-4V Substrate under Fretting Condition."
13. Magaziner, Russell L. *Examination of Contact Width on Fretting Fatigue*. MS Thesis, AFIT/GAE/ENY/02-8. Graduate School of Management and Engineering, Air Force Institute of Technology (AU), Wright-Patterson AFB OH, 2002.

14. Magaziner, Russell L. "Slip Regime Explanation of Observed Size Effects in Fretting." *Wear*. 2004; 257: 190-197.
15. Rabinowicz, E. *Friction and Wear of Materials*. New York: John Wiley and Sons Inc., 1995.
16. Ren, W., S. Mall, J. Sanders, and S.K. Sharma. "Degradation of Cu-Al Coating on Ti-6Al-4V Substrate under Fretting Conditions." *Trans. Society of Tribologists and Lubrication Engineers*. October 2003.
17. Ren, W., S. Mall, J. Sanders, and S.K. Sharma. "Evaluation of Coatings on Ti-6Al-4V Substrate under Fretting Fatigue." *Surface and Coatings Technology*. 2005; 192: 177-188.
18. Varenberg, M., G. Halperin, and I. Etsion. "Different Aspects of the Role of Wear Debris in Fretting Wear." *Wear*. 2002; 252: 902-910.
19. Waterhouse, R. B. *Fretting Corrosion*. Oxford: Pergamon Press, 1972.
20. Wittkowsky, U., P.R. Birch, J. Dominguez, and S. Suresh. "An apparatus for quantitative fretting fatigue testing." *Fatigue and Fracture Engng Mater Struct*. Blackwell Science Ltd., 1999; 22: 307-320.
21. Yaksel, Halil I. *Effects of Shot-Peening on High Cycle Fretting Fatigue Behavior of Ti-6Al-4V*. MS Thesis, AFIT/GAE/ENY/02-12. Graduate School of Management and Engineering, Air Force Institute of Technology (AU), Wright-Patterson AFB OH, 2002.

## **Vita**

Ensign Karl Murray was born in Amarillo, TX, and grew up in Rochester, MN, until he graduated from Lourdes High School in 2001. After high school, Ensign Murray entered the class of 2005 in Annapolis, MD, at the United States Naval Academy. After commissioning, he was sent directly to the Air Force Institute of Technology to earn a degree in Aeronautical Engineering. Upon graduating, Ensign Murray will head to Pensacola, FL, to begin flight training as a naval aviator.

<b>REPORT DOCUMENTATION PAGE</b>					Form Approved OMB No. 074-0188
<p>The public reporting burden for this collection of information is estimated to average 1 hour per response, including the time for reviewing instructions, searching existing data sources, gathering and maintaining the data needed, and completing and reviewing the collection of information. Send comments regarding this burden estimate or any other aspect of the collection of information, including suggestions for reducing this burden to Department of Defense, Washington Headquarters Services, Directorate for Information Operations and Reports (0704-0188), 1215 Jefferson Davis Highway, Suite 1204, Arlington, VA 22202-4302. Respondents should be aware that notwithstanding any other provision of law, no person shall be subject to an penalty for failing to comply with a collection of information if it does not display a currently valid OMB control number.</p> <p><b>PLEASE DO NOT RETURN YOUR FORM TO THE ABOVE ADDRESS.</b></p>					
<b>1. REPORT DATE (DD-MM-YYYY)</b> 05 -06-2006		<b>2. REPORT TYPE</b> Master's Thesis		<b>3. DATES COVERED (From – To)</b> Jun 2005 – Jun 2006	
<b>4. TITLE AND SUBTITLE</b>  Wear Analysis of Cu-Al Coating on Ti-6Al-4V Under Fretting				<b>5a. CONTRACT NUMBER</b>	
				<b>5b. GRANT NUMBER</b>	
				<b>5c. PROGRAM ELEMENT NUMBER</b>	
<b>6. AUTHOR(S)</b>  Murray, Karl, N., ENS, USN				<b>5d. PROJECT NUMBER</b>	
				<b>5e. TASK NUMBER</b>	
				<b>5f. WORK UNIT NUMBER</b>	
<b>7. PERFORMING ORGANIZATION NAMES(S) AND ADDRESS(S)</b>  Air Force Institute of Technology Graduate School of Engineering and Management (AFIT/EN) 2950 Hobson Way WPAFB OH 45433-7765				<b>8. PERFORMING ORGANIZATION REPORT NUMBER</b>  AFIT/GAE/ENY/06-J12	
<b>9. SPONSORING/MONITORING AGENCY NAME(S) AND ADDRESS(ES)</b>  AFRL / Materials and Manufacturing Directorate Attn: Jeffrey Sanders WPAFB, OH 45433-7817				<b>10. SPONSOR/MONITOR'S ACRONYM(S)</b>	
				<b>11. SPONSOR/MONITOR'S REPORT NUMBER(S)</b>	
<b>12. DISTRIBUTION/AVAILABILITY STATEMENT</b> APPROVED FOR PUBLIC RELEASE; DISTRIBUTION UNLIMITED.					
<b>13. SUPPLEMENTARY NOTES</b>					
<p><b>14. ABSTRACT</b></p> <p>The effects of changes in the coefficient of friction (CoF) between the contacting surfaces on the fretting wear characteristics of Cu-Al coating on Ti-6Al-4V were investigated. This Cu-Al coating is part of a system that is applied to titanium turbine blades to reduce fretting at the interface. In the application, there is a solid lubricant that is added on top of the coating as an assembly aid and to help reduce the friction while the lubricant remains within the contact. Previous studies have researched the characteristics of the coating without the additional lubricant. In this study, liquid motor oil was applied to the contact region to simulate real-world conditions with a lower CoF. To characterize the wear, several methods were used, the most useful being the accumulated dissipated energy method. The accumulated relative displacement method did not take into account the differences between the tangential forces for tests conducted at different CoF values, whereas the dissipated energy method did. The wear characteristics of tests conducted in the current study were similar to those of a previous study, conducted at a higher CoF, when analyzed with the dissipated energy method, but this was most likely due to the ambiguity of the calculated wear volumes.</p>					
<p><b>15. SUBJECT TERMS</b></p> <p>Fretting Fatigue, Fretting Wear, Lubrication, Coefficient of Friction</p>					
<b>16. SECURITY CLASSIFICATION OF:</b>		<b>17. LIMITATION OF ABSTRACT</b>	<b>18. NUMBER OF PAGES</b>	<b>19a. NAME OF RESPONSIBLE PERSON</b> Dr. Shankar Mall, AFIT (ENY)	
REPORT U	ABSTRACT U	c. THIS PAGE U	UU	75	<b>19b. TELEPHONE NUMBER</b> (Include area code) (937) 255-3636, ext 4587; e-mail: Shankar.mall@afit.edu